**US Army Corps
of Engineers**®
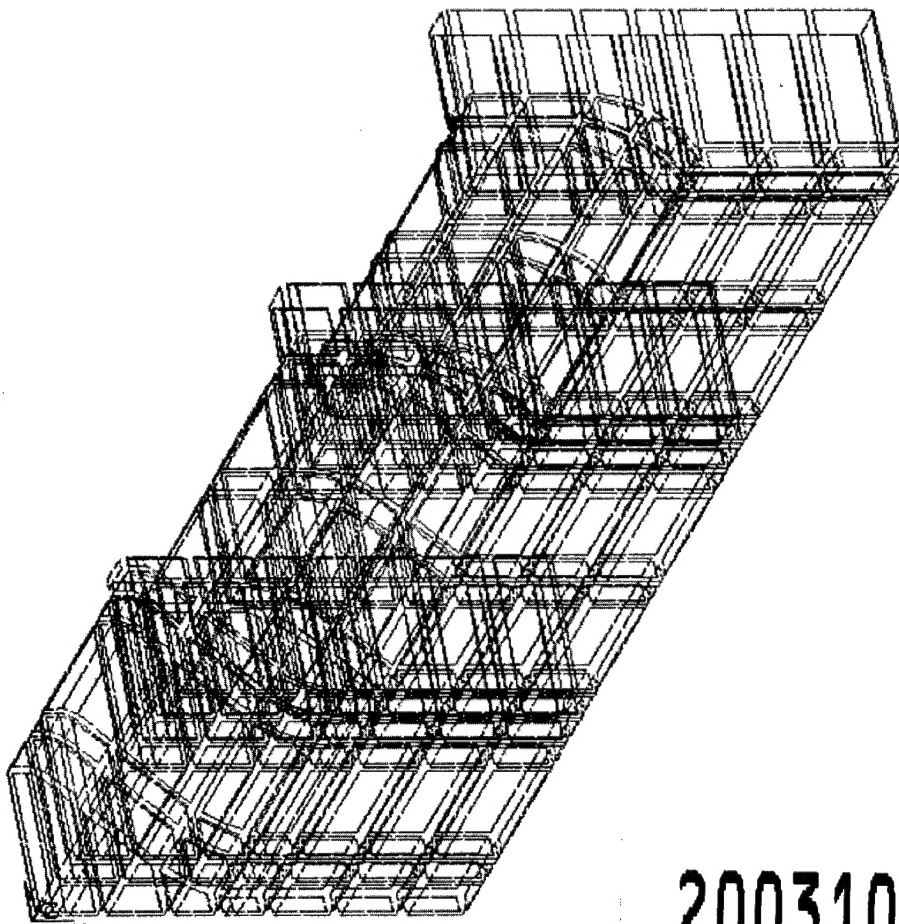Engineer Research and
Development Center

Innovations for Navigation Projects Research Program

Design by Analysis of Innovative Navigation Structures

Theoretical Manual

Kerry T. Slattery and Guillermo A. Riveros

August 2003

20031007 030

Design by Analysis of Innovative Navigation Structures

Theoretical Manual

Kerry T. Slattery

Southern Illinois University
Carbondale, IL 62901

Guillermo A. Riveros

U.S. Army Engineer Research and Development Center
Information Technology Laboratory
3909 Halls Ferry Road
Vicksburg, MS 39180-6199

Final report

ABSTRACT: This report describes the development of design by analysis methods for innovative navigation structures. The modeling approach is designed to facilitate the development of a complex three-dimensional finite element mesh and efficiently analyze the structure. Techniques to automatically generate a detailed model of the structure and perform required analysis and design calculations for the individual concrete slabs under all applied loads are illustrated, along with methods for identifying and reporting details of the design for each slab under the worst-case loading.

The two-way slab design approach (based on American Concrete Institute guidance, ACI 318-02) is summarized, along with a description of methods to calculate shear, moment, and thrust throughout the shell elements and at selected cross sections of the superelements. The design section includes the approach used to modify design parameters based on analysis results. Finally, guidelines are provided for modeling the response of soil and piles used in the foundation.

Contents

Conversion Factors, Non-SI to SI Units of Measurement

Non-SI units of measurement used in this report can be converted to SI units as follows:

Multiply	By	To Obtain
degrees (angle)	0.01745329	radians
feet	0.3048	meters
inches	25.4	millimeters
kips (force)	4.448222	kilonewtons
pounds (force) per square foot	47.88026	pascals
pounds (force) per square inch	6.894757	kilopascals
pounds (mass) per cubic foot	16.01846	kilograms per cubic meter
square feet	0.09290304	square meters
square inches	6.4516	square centimeters

Preface

The work described in this report was authorized by Headquarters, U.S. Army Corps of Engineers (HQUSACE), as part of the Innovations for Navigation Projects (INP) Research Program. The study was conducted under Work Unit (WU) 33273, "Integrated Design and Analysis System for Navigation Structures," managed at the U.S. Army Engineer Research and Development Center (ERDC), Vicksburg, MS.

Dr. Tony C. Liu was the INP Coordinator at the Directorate of Research and Development, HQUSACE; Research Area Manager was Mr. Barry Holliday, HQUSACE; and Program Monitors were Mr. Mike Kidby and Ms. Anjana Chudgar, HQUSACE. Mr. William H. McAnally of the ERDC Coastal and Hydraulics Laboratory was the Lead Technical Director for Navigation Systems; Dr. Stanley C. Woodson, ERDC Geotechnical and Structures Laboratory, was the INP Program Manager.

This report was prepared by Dr. Kerry T. Slattery of the Southern Illinois University and Mr. Guillermo A. Riveros of the Engineering and Informatics Systems Division (EISD), ERDC Information Technology Laboratory (ITL). The work was monitored by Mr. Riveros, Principal Investigator of WU 33273, under the supervision of Dr. Charles R. Welch, Chief, EISD; and Dr. Jeffery P. Holland, Director, ERDC ITL.

Commander and Executive Director of ERDC was COL James R. Rowan, EN. Dr. James R. Houston was Director.

1 Introduction

This report is a theoretical manual that describes the development of "design by analysis" methods for innovative navigation structures. The modeling approach is designed to facilitate the development of a complex three-dimensional finite element mesh and efficiently analyze the structure. Techniques to automatically generate a detailed model of the structure and perform required analysis and design calculations for the individual concrete slabs under all applied loads are illustrated, along with methods for identifying and reporting details of the design for each slab under the worst-case loading.

This manual begins with a description of assumptions made concerning in-the-wet construction techniques and how these assumptions are accounted for in this development. The section on modeling considerations documents the methods used to replicate typical details of the float-in segments. The finite element formulation for the two element types is then presented. Shell elements are used to model the individual concrete slabs. These are connected with superelements derived to provide an accurate solid model of the joint details, including tapers between slabs. An innovative approach to efficiently calculate the stiffness matrix and the slave-master transformation matrix for an arbitrary joint geometry is introduced.

The two-way slab design approach (based on American Concrete Institute requirements, ACI 318-02) is summarized, along with a description of methods to calculate shear, moment, and thrust throughout the shell elements and at selected cross sections of the superelements. The design section includes the approach used to modify design parameters based on analysis results. Finally, guidelines are provided for modeling the response of soil and piles used in the foundation. Design algorithms are presented in Appendix A.

2 In-the-Wet Construction Approach

Traditional methods to construct massive concrete navigation structures have required the placement of a cofferdam to dewater the construction site. Several Corps of Engineers projects are currently in various stages of design and construction using new methods in which a concrete shell is constructed in a dry dock, floated to the placement site, and lowered on a prepared underwater foundation. This "in-the-wet" construction approach will save much of the time and expense of cofferdam construction.

The fabrication of a concrete shell that is light enough to float and strong enough to resist substantial pressure from water and tremie concrete during construction requires careful planning and design. The development of "design by analysis" (DBA) methods is based on the approach being used in the Pittsburgh District's Braddock Dam, which reflects experience gained in other applications by the consultants on the project. The following design assumptions are used in the DBA application.

2.1 Shell Layout Assumptions

The floating structure is primarily reinforced concrete. A local coordinate system is defined so that concrete diaphragm walls are arranged along section lines in both the E-W and N-S directions. The local coordinate system is defined such that water flows through the structure from north to south. Even though the height and thickness of the walls may vary along the length of the segment, diaphragm walls must be placed continuously, centered on the section lines. Figure 2.1 shows a plan-view cross section of the Braddock Dam. Steel stiffeners may be placed between large wall panels to provide support for external pressure loads.

2.2 Diaphragm Panel Construction

The diaphragm walls are precast flat with reinforcing steel protruding to develop a connection at the joints. They are arranged and supported in their designed location before the bottom slab and the joints are cast in place. Some
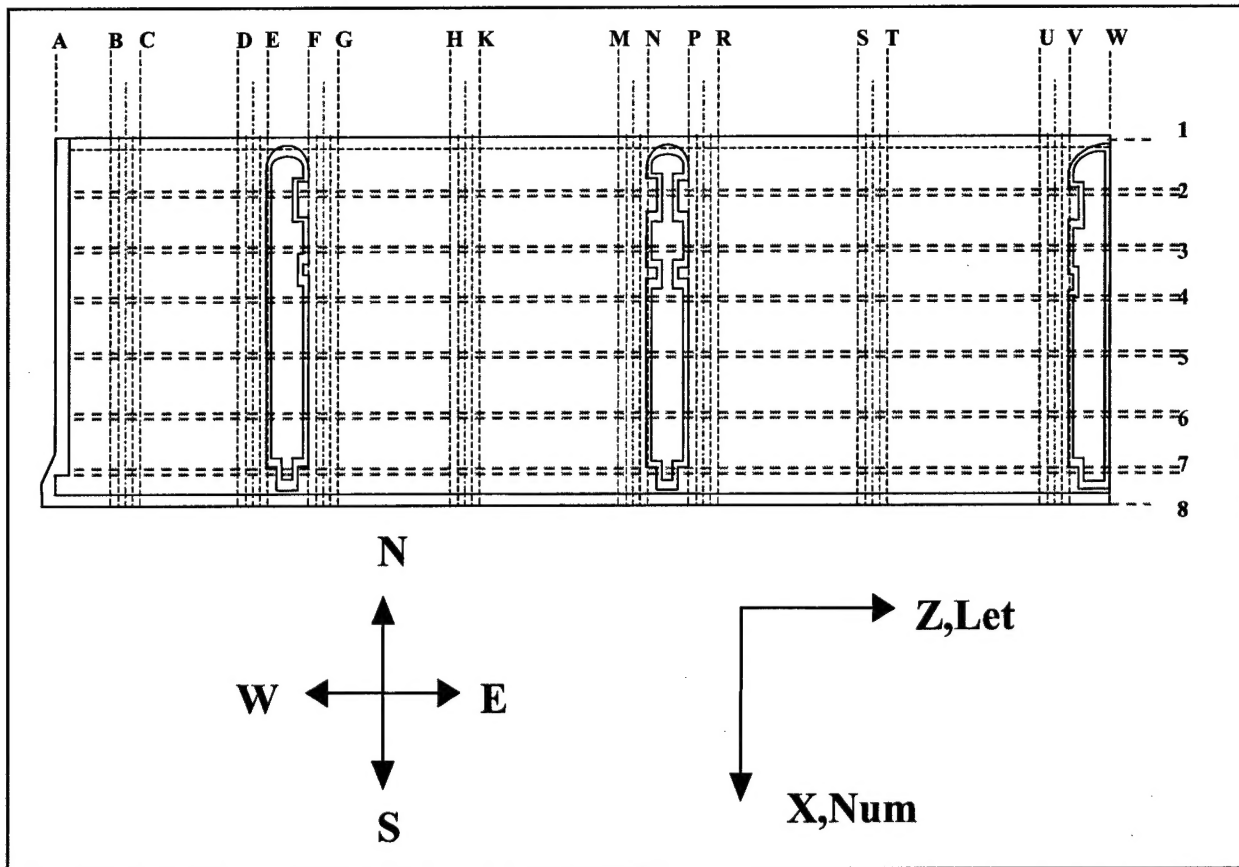
Figure 2.1. Plan view of Braddock Dam

taper is required at most joints to provide a stiffer, stronger section where the moment and shear loads are greatest and to provide adequate space for the confining reinforcement. This design should be standardized as much as possible in order to reuse formwork. Figure 2.2 shows a typical vertical joint placement.

2.3 Critical Load Cases

Critical loads for most components of the structure occur when the fluid levels in adjacent cells are substantially different, resulting in a large differential hydrostatic pressure on the concrete slab. The load cases must be developed in concert with the construction planner in order to identify all significant planned and accidental events. Each concrete slab must be designed for both positive and negative moments along both slab axes.

Critical loads cases defined for the Braddock Dam were these:

a. Float-out.

b. Outfitting yard.

c. Accidental flood event.

d. Touch-down.

e. Flood event.

f. Dead load.

g. Pier wall in-fill.

h. Dewater bay.

i. Second-stage casting.
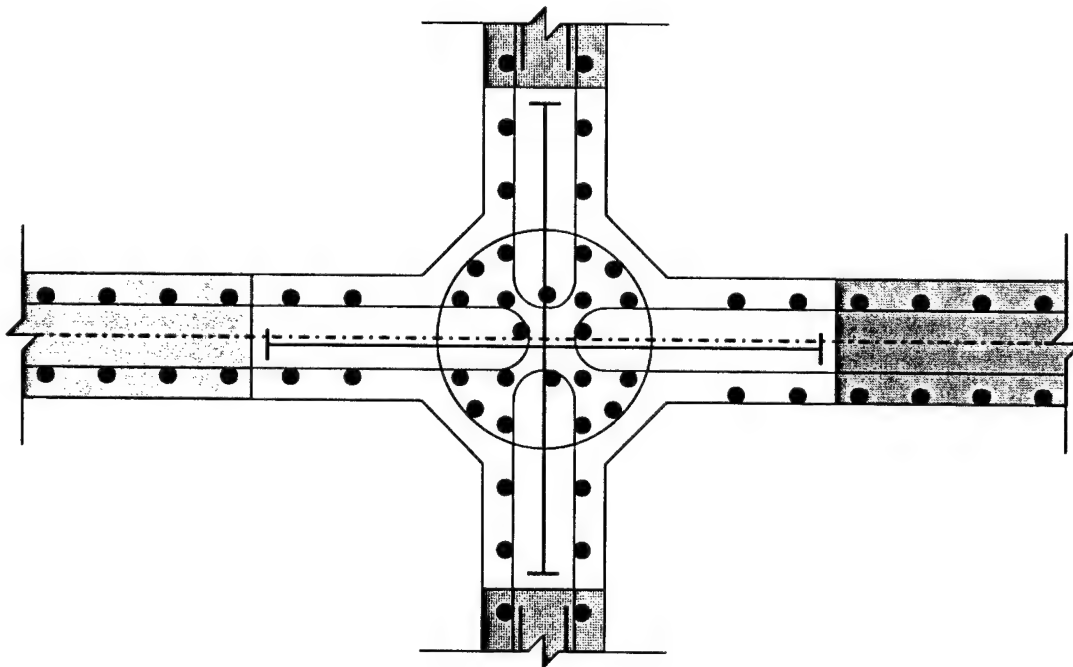
Figure 2.2. Typical vertical joint

2.4 Boundary Conditions

Four boundary conditions must be modeled in the typical float-in structure: continuous elastic foundation, floating, set-down shafts, and drilled piers. One or, in some cases, two or three of these conditions are in effect at any given time. Set-down shafts and drilled piers are similar in their design and function with the exception that only set-down shafts are engaged when the structure is initially lowered to the bottom of the river.

The continuous elastic foundation may exist during initial fabrication in the dry dock or after the segment is placed on the set-down shafts in the river and

grouted. Standard finite element approaches are available for shell elements on an elastic foundation (Chandrupatla and Belegundu 1997). The approximate stiffness of the soil or grout in place is a required modeling parameter. The force applied to a structure resting on an elastic foundation is proportional to the deflection of the bottom of the structure; thus, differential settlement is expected. Typically, the upstream end of a navigation structure is deeper, so it will have a greater weight per square foot of plan area.

The segment will be floating from the time the dry dock is flooded until it is placed on the set-down shafts. The pressure applied to the outside of the structure is a function of the draft (the depth of the bottom of the structure when floating). The draft is based on the buoyancy of the structure and can be calculated as

$$D = \frac{Total\ weight}{Plan\ area \times Water\ density} \tag{2.1}$$

Pressure is exerted on all submerged faces of the structure. The magnitude of the pressure is proportional to the depth. A substantial horizontal pressure can be expected on the outside walls of the structure, which is not present when the structure is supported on an elastic foundation. A finite element model of a floating structure should be in equilibrium if the pressure is input exactly; however, minimal restraint is required and is applied by including springs at the four corners of the model. The construction planner must ballast the structure to account for higher weight per square foot on the upstream end of the structure so that the segment floats in a level position.

The structure is initially set on a limited number of drilled piers. These are identified as set-down drilled shafts. Additional drilled piers are distributed under the segment. Precast holes in the bottom slab are placed over drilled piers. These provide lateral and vertical support after the hole is grouted. These shafts in a typical structure are reinforced concrete on the order of 6 ft[1] in diameter. The shafts can be modeled as springs with one stiffness value in the vertical direction and another in the horizontal direction. The horizontal stiffness of a round pier is the usually the same in any direction. The vertical stiffness is a function of the stiffness of the pier itself, the foundation material at the bottom of the shaft, and any support gained from skin friction. The translational stiffness is controlled by the flexural stiffness of the reinforced concrete shaft and support from the surrounding soil. Methods for calculating these values are outlined by the CASE Task Group on Pile Foundations (Office, Chief of Engineers (OCE) 1983).

---

[1] A table of factors for converting non-SI units of measurement to SI units is presented on page v.

3 Modeling Considerations

3.1 Assumptions

The structural designer must know the overall dimensions of the segment, the location and width of piers, and the shape of the individual spillways between piers. The designer may have a preliminary layout for the internal diaphragm walls. These walls are required to support the external slab in order to produce an efficient structure. Spacing between diaphragm walls is usually fairly uniform across a segment. Diaphragms should be spaced to break the slabs into sections that are nearly square, in order to produce two-way slab action. Individual walls may be placed to coincide with changes in the geometry of spillways. Diaphragm walls are closely spaced where the segment rests on drilled shafts to distribute the concentrated loads. The side walls of a pier will be aligned with diaphragm walls.

3.2 Spillway Shapes

Spillway layout requires the selection of a template of a standard spillway shape. The standard spillway shapes are based on typical Corps of Engineers designs. The template approach assumes that, for example, the outline of the typical fixed-crest weir is composed of the same series of geometrical entities–flat bottom with flat ends having a radius at the corners and at transitions between flat sections on the top surface. The template fits the geometry of the segment to the overall dimensions of the structure by extending the length of the level area on the downstream end of the spillway to the predetermined length of the segment. A minimum number of changeable parameters are used to describe the geometry. The other dimensions of the spillway are calculated using basic geometrical relationships without changing the essential shape of the spillway. Figure 3.1 shows the parameters required to describe the shape of a typical fixed-crest weir.

The spillway shape can change only at a pier. The standard design approach for a pier placed where the spillway shape changes is to extend both spillways into the pier. For example, the Braddock Dam segment shown in Figure 2.1 has three spillway shapes. The pier between section lines E and F transitions from the fixed-crest weir to the water quality gate bay. This can create complex geometry for modeling, especially when the top surface of the two shapes intersects at one or more points.
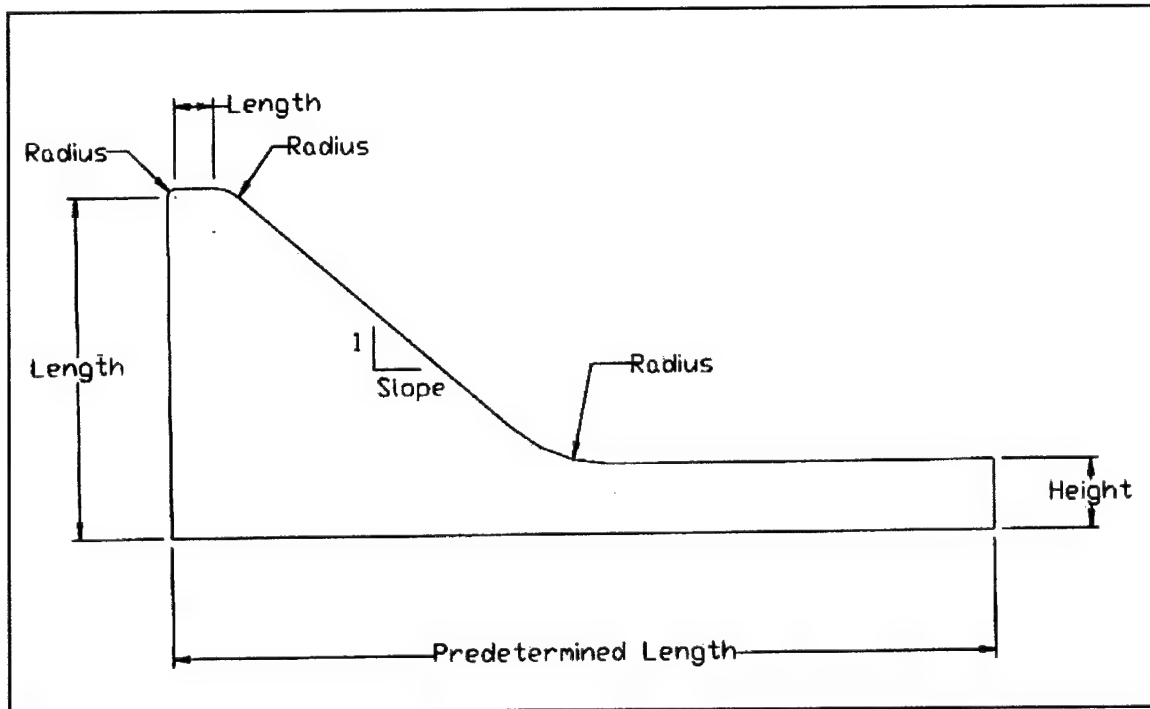
Figure 3.1. Fixed-crest weir template

3.3 Tapers

Tapers are typically specified at points where slabs intersect at angles near 90 deg. They are used to stiffen the slab where the highest moment and shear loads occur. The superelement formulation requires at least a minimal taper at all corners in order to map superelement nodes to unique shell nodes. Tapers are defined by the terms "rise" and "run." These terms are loosely applied because they actually define dimensions relative to surfaces and center lines, as shown in Figure 3.2. The location of the taper focal point (TFP) is defined by these rise and run parameters. The run is the distance from the center of the diaphragm wall to the TFP, and the rise is the distance normal to the outside surface of the spillway. The toe of the taper is on the line normal to the outside surface through the TFP, as shown. The rise is measured parallel to that line.

To enforce uniformity in the segment layout and finite element model, the rise and run values are constrained. Adjacent tapers must be consistent; that is, the run must be the same for both the top and bottom taper on one side of a diaphragm wall. The run can be different on the left and right side of a diaphragm wall. Only one rise value is permitted along the bottom. A different value may be applied to tapers on the top.
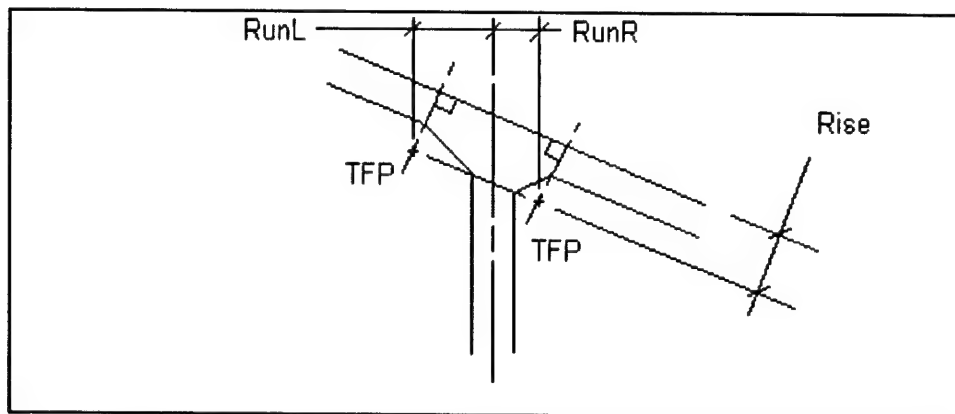
Figure 3.2. Taper dimension definition

3.4 Piers

Piers extend above the spillway surface to some constant elevation. The walls coincide with adjacent diaphragm walls along lettered (N-S) section lines (Figure 2.1). The ends are enclosed. The upstream end is usually curved for smoother flow. The downstream end may be stepped to hold temporary steel gates used to float the segment. The ends of pier walls are modeled as flat walls to simplify the model.

When the designer designates the location of a pier wall along a section line, the finite element model is divided at that line. The shells and superelements that would normally be generated along the section line are divided into two appropriate elements. Figure 3.3 shows the finite element configuration for a simple model with a pier wall. Figure 3.3a is an isometric view of the segment layout. The view from the downstream end (Figure 3.3b) shows the shell elements in the model. The finite element model is divided into three parts (A, B, and C). Figure 3.3c is the end view of the model with the superelements. The boundaries are not as clear in this sketch, but each superelement is actually two separate elements.

The resulting finite element model for the segment begins as several separate segments that must then be tied together in the finite element model. The tying operation involves identifying all shell nodes next to the interface and designating one set as masters and the other as slaves. Master nodes and elements are those on the local west side (-Z) of the center line. Slaves are on the local east side (+Z). Since the spillway geometry may be different on the two sides at the pier wall, these nodes will generally not line up. However, they may fall on coincident vertical lines since the diaphragm locations will be consistent. The slave node degrees of freedom are mapped to the master elements by (a) determining which element would enclose a node if it were translated to the plane of the master elements, (b) calculating the local coordinates of the node location, and (c) developing a transformation matrix to map slave node displacements to the master element.
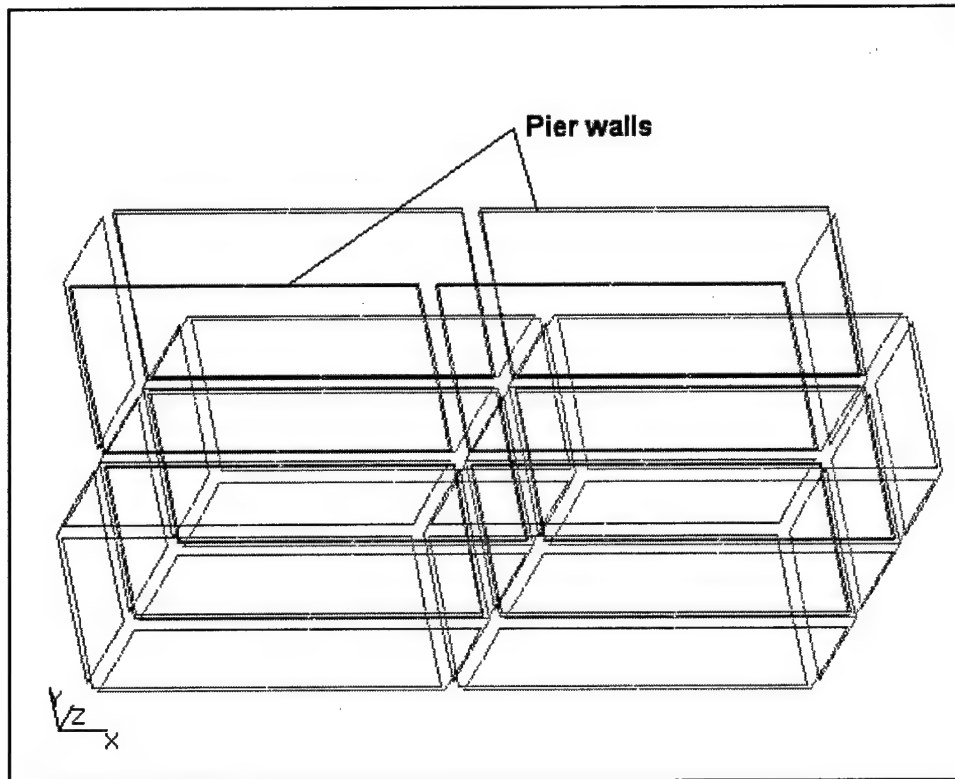
a. Isometric view of segment layout

Figure 3.3. Finite element configuration for a simple model with pier wall
(Sheet 1 of 3)
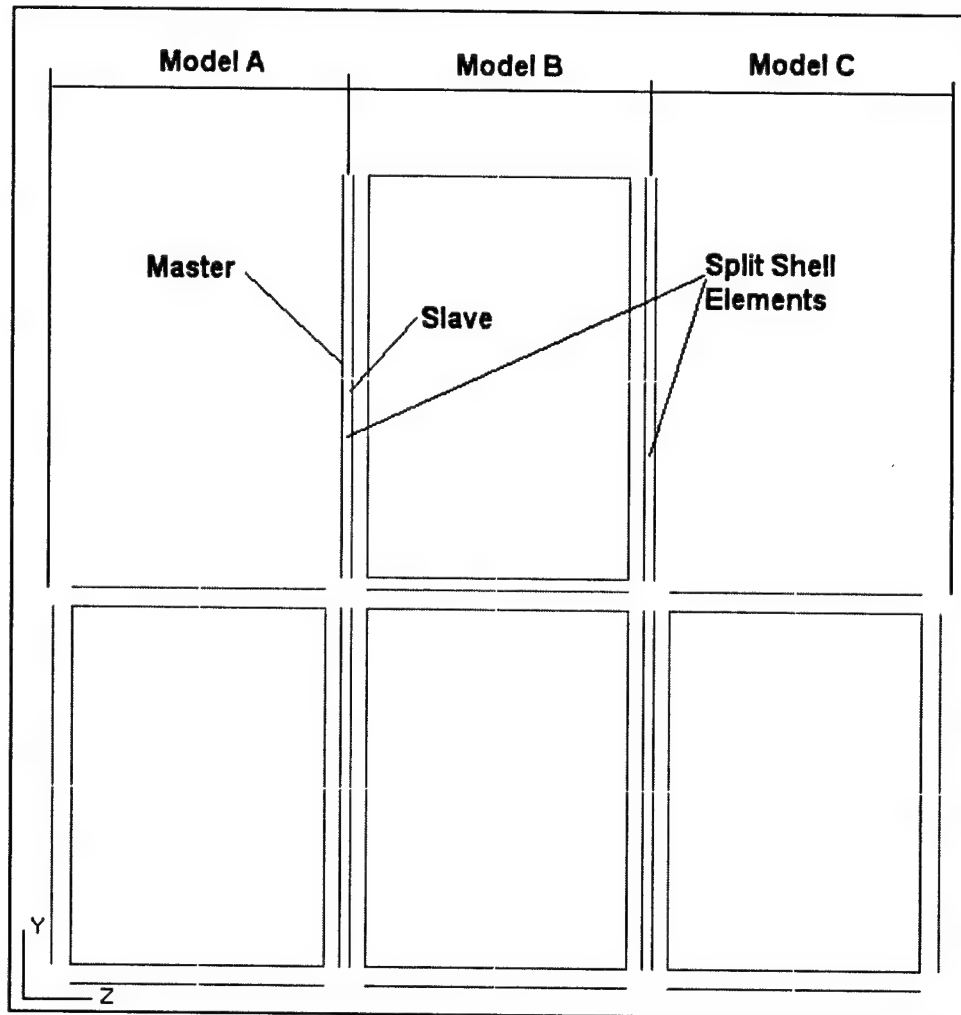
b. View from south end showing three submodels

Figure 3.3. (Sheet 2 of 3)

Model A   Model B   Model C

Separate
Superelements
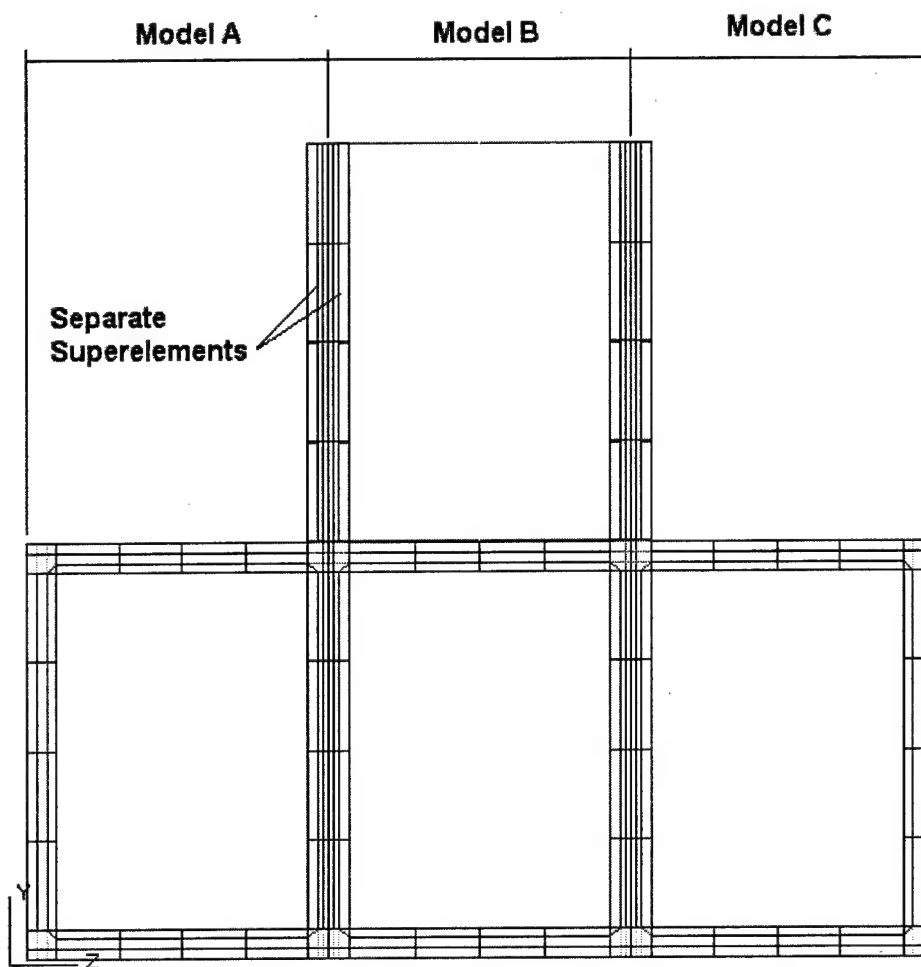
c. View from local south end (X) with solid joint elements

Figure 3.3. (Sheet 3 of 3)

Figure 3.4 shows a slave node located within the master element with node numbers 1-8. The Z coordinate of the slave node is one half the thickness of the concrete slab from that of the master element. The local coordinates in the master element, ξ and η, are found by inverting the shape functions for the shell element iteratively.

The transformation to calculate the deflection at the slave node, given the deflections of the nodes in the master element, is developed in two steps. The first is to find the deflection of a point on the midplane of the master element adjacent to the slave node using the standard shape function relationship (see Section 4.1). The deflection of the slave node is then mapped to that point by

$$\{u_s\} = \left[T_{node}\right]\{u_m\}$$

where (3.1)

$$
\begin{Bmatrix} u_s \\ v_s \\ w_s \\ \alpha_s \\ \beta_s \end{Bmatrix} = \begin{bmatrix} 1 & 0 & 0 & 0 & -\dfrac{t_i}{2} \\ 0 & 1 & 0 & \dfrac{t_i}{2} & 0 \\ 0 & 0 & 1 & 0 & 0 \\ 0 & 0 & 0 & 1 & 0 \\ 0 & 0 & 0 & 0 & 1 \end{bmatrix} \begin{Bmatrix} u_m \\ v_m \\ w_m \\ \alpha_m \\ \beta_m \end{Bmatrix}
$$

where subscript s refers to slave degrees of freedom, and subscript m refers to masters. The thickness of the slab is t. The rotations at the two points are equal, to enforce the assumption that plane sections remain plane in a shell element.
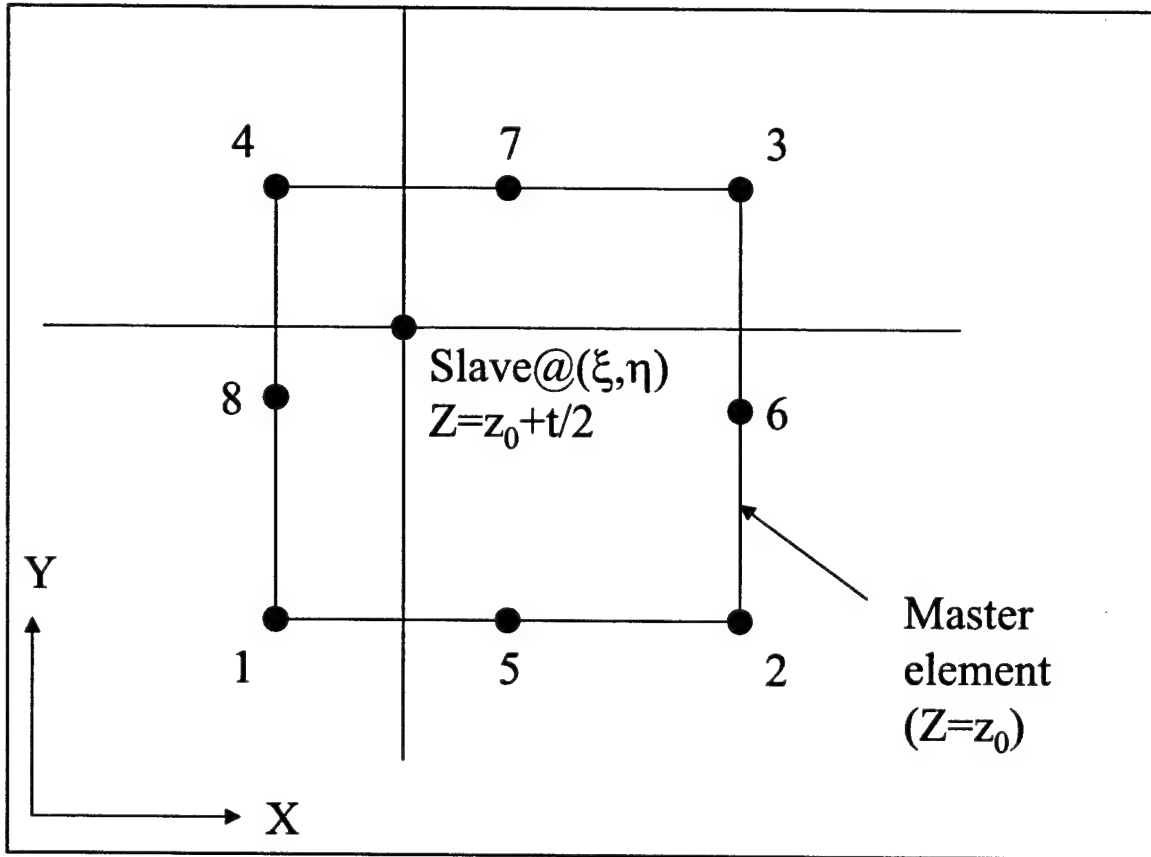
Figure 3.4. Slave node is mapped in to master element

Slave nodes are eliminated from the finite element solution, and the stiffness matrix for elements containing slave nodes is transformed to align with the master degrees of freedom by developing a transformation matrix for all degrees of freedom in elements with slave nodes using the transformations described above. The deflections at each slave nodes are a function of the deflections at up

to eight master nodes. The transformation matrix, [T$_{elem}$], is assembled from [T$_{node}$] submatrices weighted by the shape functions relative to the master node.

$$\{u_s\} = [T_{elem}]\{u_m\}$$ (3.2)

The stiffness matrix for the slave element is then calculated from

$$[K_{master}] = [T_{elem}]^T [K_{slave}][T_{elem}]$$ (3.3)

3.5   Loading

Loads on the structure include gravity loads imposed as body forces on the elements, external pressures applied inside the cells or on the outside walls of the structure, and concentrated loads that can be applied to nodes. Body forces are calculated at the integration points and distributed to the nodes by

$$\{P_b\} = 2\int_{-1}^{1}\int_{-1}^{1}\{f\}^T b_y|J|d\xi d\eta$$ (3.4)

Hydrostatic pressure loads are defined for various load cases by designating the fluid level in each cell or external face relative to the bottom of the structure (Y = 0). The fluid may be water or tremie concrete. When a hydrostatic pressure is imposed on a shell element, the depth of the integration point is calculated relative to the top of the fluid, and the pressure is calculated by multiplying the depth by the density of the fluid. This pressure is then distributed to the nodes using the shape functions by

$$\{P_{pr}\} = 2\int_{-1}^{1}\int_{-1}^{1}\{f\}^T p(y_i)|J|d\xi d\eta$$ (3.5)

The total pressure is distributed to the x, y, and z directions by multiplying by the direction cosines.

This approach assumes that the pressure varies linearly in the vertical direction. This, of course, is not exact when the top of the fluid is in the middle of an element. In this case, the pressures at the integration points are adjusted to impose the same total force but distribute it across the entire element. The moment will tend to be greater in this case, but the errors decrease as the finite element mesh is refined.

4   Shell Element Formulation

An eight-node, 40-degrees of freedom (DOF), biquadratic shell element is used to model the concrete slabs. The formulation follows Weaver and Johnston (1984). The global finite element model uses six DOF per node. Stiffness at the translation degrees of freedom is calculated directly in the global coordinate system using a transformed materials property matrix. The local rotational DOF, α and β, are transformed based on the direction cosines at each node.

4.1   Geometry

Figure 4.1 shows the node numbering and natural (ξ, η, ζ) coordinate system for the element. The two rotational DOF, α and β, are aligned with the local x' and y' directions of the element at any point. The z' direction is normal to the midplane of the element. The x' and y' directions are perpendicular to z' and to each other at any point.

The local coordinate directions are stored as direction cosines at the nodes and integration points. These are used throughout the finite element formulation. The direction cosines are designated as

$$[V] = \begin{bmatrix} \ell_1 & \ell_2 & \ell_3 \\ m_1 & m_2 & m_3 \\ n_1 & n_2 & n_3 \end{bmatrix} \tag{4.1}$$

where ℓ_i, m_i, and n_i are the x, y, and z components of the unit vector V_i. In this formulation, V_3 is normal to the midplane of the shell, and V_1 and V_2 are aligned with the midplane normal to V_3 and to each other.

The location of any point in the element can be calculated from the natural coordinates as

$$\begin{bmatrix} x \\ y \\ z \end{bmatrix} = \sum_{i=1}^{8} f_i \begin{bmatrix} x_i \\ y_i \\ z_i \end{bmatrix} + \sum_{i=1}^{8} f_i \zeta \frac{t_i}{2} \begin{bmatrix} l_{3i} \\ m_{3i} \\ n_{3i} \end{bmatrix} \tag{4.2}$$
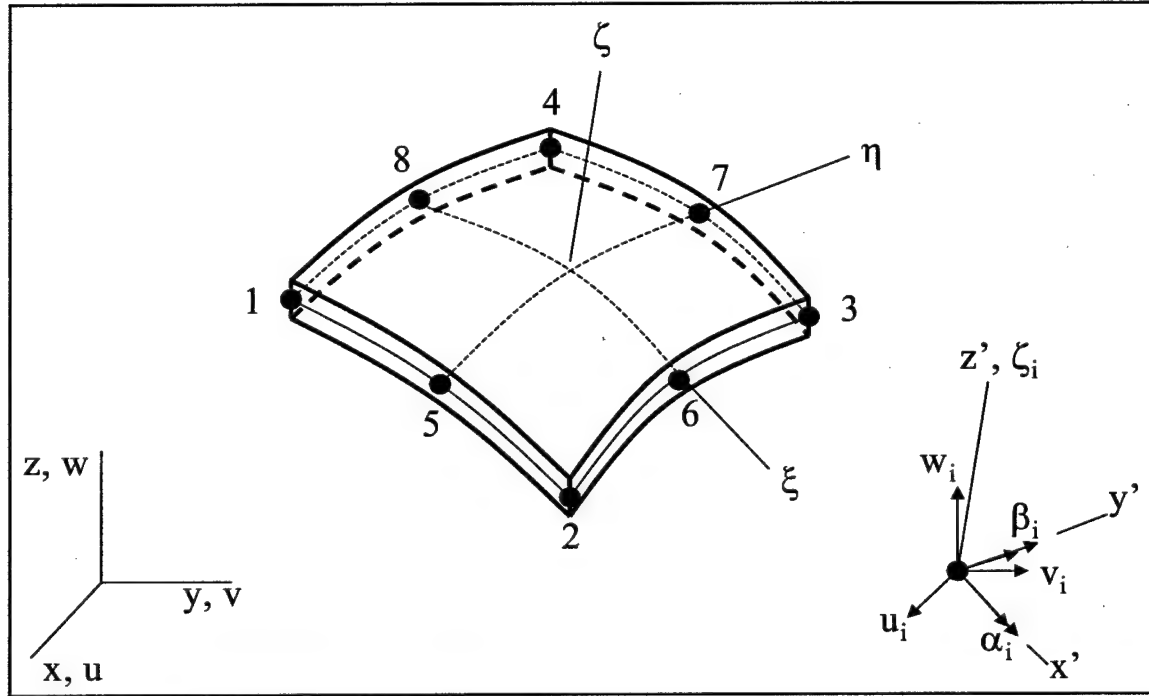
Figure 4.1. Shell element

where the shape functions f_i are functions only of the in-plane coordinates.

i	f_i	$f_{i,\xi}$	$f_{i,\eta}$
1	$(1-\xi)(1-\eta)(-\xi-\eta-1)/4$	$(2\xi+\eta)(1-\eta)/4$	$(1-\xi)(2\eta+\xi)/4$
2	$(1+\xi)(1-\eta)(\xi-\eta-1)/4$	$(2\xi-\eta)(1-\eta)/4$	$(1+\xi)(2\eta-\xi)/4$
3	$(1+\xi)(1+\eta)(\xi+\eta-1)/4$	$(2\xi+\eta)(1+\eta)/4$	$(1+\xi)(2\eta+\xi)/4$
4	$(1-\xi)(1+\eta)(-\xi+\eta-1)/4$	$(2\xi-\eta)(1+\eta)/4$	$(1-\xi)(2\eta-\xi)/4$
5	$(1-\xi^2)(1-\eta)/2$	$-\xi(1-\eta)$	$-(1-\xi^2)/2$
6	$(1+\xi)(1-\eta^2)/2$	$(1-\eta^2)/2$	$-(1+-\xi)\,\eta$
7	$(1-\xi^2)(1+\eta)/2$	$-\xi(1+\eta)$	$(1-\xi^2)/2$
8	$(1-\xi)(1-\eta^2)/2$	$-(1-\eta^2)/2$	$-(1-\xi)\,\eta$

Similarly, displacements are

$$\begin{bmatrix} u \\ v \\ w \end{bmatrix} = \sum_{i=1}^{8} f_i \begin{bmatrix} u_i \\ v_i \\ w_i \end{bmatrix} + \sum_{i=1}^{8} f_i \zeta \frac{t_i}{2} \begin{bmatrix} -l_{2i} & l_{1i} \\ -m_{2i} & m_{1i} \\ -n_{2i} & n_{1i} \end{bmatrix} \begin{bmatrix} \alpha_i \\ \beta_i \end{bmatrix} \qquad (4.3)$$

4.2 Stiffness

The derivation of the stiffness matrix follows typical finite element procedures. The Jacobian matrix for a three-dimensional element is

$$[J] = \begin{bmatrix} x,_\xi & y,_\xi & z,_\xi \\ x,_\eta & y,_\eta & z,_\eta \\ x,_\zeta & y,_\zeta & z,_\zeta \end{bmatrix} \tag{4.4}$$

The 3×3 Jacobian matrix is inverted to find the derivatives of the natural coordinates in terms of the global coordinate

$$[J^*] = \begin{bmatrix} \xi,_x & \eta,_x & \zeta,_x \\ \xi,_y & \eta,_y & \zeta,_y \\ \xi,_z & \eta,_z & \zeta,_z \end{bmatrix} \tag{4.5}$$

The strain-displacement matrix is derived by defining individual strain components in terms of the partial derivatives of the displacements.

$$\varepsilon = \begin{bmatrix} \varepsilon_x \\ \varepsilon_y \\ \varepsilon_z \\ \gamma_{xy} \\ \gamma_{yz} \\ \gamma_{zx} \end{bmatrix} = \begin{bmatrix} u,_x \\ v,_y \\ w,_z \\ u,_y + v,_x \\ v,_z + w,_y \\ w,_x + u,_z \end{bmatrix} \tag{4.6}$$

A 6×5 submatrix of the 6×40 strain-displacement matrix is then

$$[B_i] = \begin{bmatrix} a_i & 0 & 0 & -d_i \ell_{2i} & d_i \ell_{1i} \\ 0 & b_i & 0 & -e_i m_{2i} & e_i m_{1i} \\ 0 & 0 & c_i & -g_i n_{2i} & g_i n_{1i} \\ b_i & a_i & 0 & -e_i \ell_{2i} - d_i m_{2i} & e_i \ell_{1i} + d_i m_{1i} \\ 0 & c_i & b_i & -g_i m_{2i} - e_i n_{2i} & g_i m_{1i} + e_i n_{1i} \\ c_i & 0 & a_i & -d_i n_{2i} - g_i \ell_{2i} & d_i n_{1i} + g_i \ell_{1i} \end{bmatrix} \tag{4.7}$$

$$(i = 1, 2, ..., 8)$$

where

$$a_i = J_{11}^* f_{i,\xi} + J_{12}^* f_{i,\eta} \qquad d_i = \frac{t_i}{2}\left(a_i\zeta + J_{13}^* f_i\right)$$

$$b_i = J_{21}^* f_{i,\xi} + J_{22}^* f_{i,\eta} \qquad e_i = \frac{t_i}{2}\left(b_i\zeta + J_{23}^* f_i\right)$$

$$c_i = J_{31}^* f_{i,\xi} + J_{32}^* f_{i,\eta} \qquad g_i = \frac{t_i}{2}\left(c_i\zeta + J_{33}^* f_i\right)$$

The stress-strain relationship (Equation 4.8) is a function of the Young's modulus (E) and shear modulus (G) of the material. The third row and column are zero in the local coordinate system because there is no stress through the thickness (plane stress assumption).

$$\{\sigma'\} = [E'][\varepsilon']$$

or, (4.8)

$$\begin{bmatrix} \sigma_{x'} \\ \sigma_{y'} \\ \sigma_{z'} \\ \tau_{x'y'} \\ \tau_{y'z'} \\ \tau_{z'x'} \end{bmatrix} = \begin{bmatrix} E_{x'x'} & E_{x'y'} & 0 & 0 & 0 & 0 \\ E_{y'x'} & E_{y'y'} & 0 & 0 & 0 & 0 \\ 0 & 0 & 0 & 0 & 0 & 0 \\ 0 & 0 & 0 & G_{x'y'} & 0 & 0 \\ 0 & 0 & 0 & 0 & \dfrac{G_{y'z'}}{1.2} & 0 \\ 0 & 0 & 0 & 0 & 0 & \dfrac{G_{z'x'}}{1.2} \end{bmatrix} \begin{bmatrix} \varepsilon_{x'} \\ \varepsilon_{y'} \\ \varepsilon_{z'} \\ \gamma_{x'y'} \\ \gamma_{y'z'} \\ \gamma_{z'x'} \end{bmatrix}$$

This relationship is transformed to the global coordinate system by

$$[E] = [T_\varepsilon]^T [E'][T_\varepsilon]$$ (4.9)

where

$$T_\varepsilon = \begin{bmatrix} l_1^2 & m_1^2 & n_1^2 & l_1 m_1 & m_1 n_1 & n_1 l_1 \\ l_2^2 & m_2^2 & n_2^2 & l_2 m_2 & m_2 n_2 & n_2 l_2 \\ l_3^2 & m_3^2 & n_3^2 & l_3 m_3 & m_3 n_3 & n_3 l_3 \\ 2l_1 l_2 & 2m_1 m_2 & 2n_1 n_2 & l_1 m_2 + l_2 m_1 & m_1 n_2 + m_2 n_1 & n_1 l_2 + n_2 l_1 \\ 2l_2 l_3 & 2m_2 m_3 & 2n_2 n_3 & l_1 m_2 + l_2 m_1 & m_2 n_3 + m_3 n_2 & n_2 l_3 + n_3 l_2 \\ 2l_3 l_1 & 2m_3 m_1 & 2n_3 n_1 & l_1 m_2 + l_2 m_1 & m_3 n_1 + m_1 n_3 & n_3 l_1 + n_1 l_3 \end{bmatrix}$$ (4.10)

Finally, the stiffness matrix is calculated by integrating $[B]^T[E][B]$ over the volume of the element. This operation must be performed by numerical integration by summing the values at the integration points. Four integration points are used in the current formulation. These are on the midplane ($\zeta = 0$). The in-plane natural coordinates of the four points are

$$\xi_1 = -\frac{1}{\sqrt{3}} \quad \eta_1 = -\frac{1}{\sqrt{3}}$$

$$\xi_2 = \frac{1}{\sqrt{3}} \quad \eta_2 = -\frac{1}{\sqrt{3}}$$

$$\xi_3 = \frac{1}{\sqrt{3}} \quad \eta_3 = \frac{1}{\sqrt{3}}$$

$$\xi_4 = -\frac{1}{\sqrt{3}} \quad \eta_4 = \frac{1}{\sqrt{3}}$$

(4.11)

The strain-displacement matrix is divided into two components to separate out the terms containing the ζ term:

$$[B] = [B_a] + \zeta[B_b]$$

The stiffness matrix as calculated by Equation 4.13:

$$[K] = \sum_{i=1}^{4} \left(2\left[B_a(\xi_i, \eta_i)\right]^T [E]\left[B_a(\xi_i, \eta_i)\right] + \frac{2}{3}\left[B_b(\xi_i, \eta_i)\right]^T [E]\left[B_b(\xi_i, \eta_i)\right] \right) \\ \left| J(\xi_i, \eta_i) \right| W_i$$

(4.13)

4.3   Load Boundary Conditions

4.3.1 Body forces

Body forces are due to gravity in the negative Y direction. Equivalent nodal loads due to gravity body forces with a material density, b_y, are

$$\begin{Bmatrix} P_{1y} \\ P_{2y} \\ P_{3y} \\ P_{4y} \\ P_{5y} \\ P_{6y} \\ P_{7y} \\ P_{8y} \end{Bmatrix} = 2\sum_{i=1}^{4} \begin{Bmatrix} f_1(\xi_i, \eta_i) \\ f_2(\xi_i, \eta_i) \\ f_3(\xi_i, \eta_i) \\ f_4(\xi_i, \eta_i) \\ f_5(\xi_i, \eta_i) \\ f_6(\xi_i, \eta_i) \\ f_7(\xi_i, \eta_i) \\ f_8(\xi_i, \eta_i) \end{Bmatrix} b_y |J| W_i$$

(4.14)

4.3.2 Pressure

When pressure is applied to an element face, the equivalent nodal forces are determined based on the pressure function at the integration points. The total force at the node is calculated as

$$
\begin{Bmatrix} P_{1y} \\ P_{2y} \\ P_{3y} \\ P_{4y} \\ P_{5y} \\ P_{6y} \\ P_{7y} \\ P_{8y} \end{Bmatrix} = \sum_{i=1}^{4} \begin{Bmatrix} f_1(\xi_i,\eta_i) \\ f_2(\xi_i,\eta_i) \\ f_3(\xi_i,\eta_i) \\ f_4(\xi_i,\eta_i) \\ f_5(\xi_i,\eta_i) \\ f_6(\xi_i,\eta_i) \\ f_7(\xi_i,\eta_i) \\ f_8(\xi_i,\eta_i) \end{Bmatrix} P(y_i)|J|W_i
\tag{4.15}
$$

Pressure components in the x, y, and z directions are determined by multiplying the $P(y_i)$ by the direction cosines at the integration point.

If an element is only partially submerged, this approach would accurately model the linearly varying positive pressure, but it would effectively apply a negative pressure to the element above the fluid. A simple approximation is employed to adjust the nodal loads to duplicate the total pressure force on the element without creating negative pressures. The node with the greatest elevation is determined for the element. The fluid level is assumed to be at this point, and the density of the fluid is reduced to exert the same force.

For example, a rectangular shell element is 20 ft wide. The elevation at the bottom of the element is 10 ft, and the elevation is 25 ft at the top. The fluid level is 20 ft of water with a density of 62.4 pcf. The total pressure force on the element is

$$P = (20 \text{ ft}) (20 \text{ ft} - 10 \text{ ft}) (10 \text{ ft} \times 62.4 \text{ lb/ft}^3)/2 = 62{,}400 \text{ lb}$$

Multiplying the density by $\left(\dfrac{20'-10'}{25'-10'}\right)^2 = \dfrac{4}{9}$ reduces the density to 27.7 pcf and imposes the same force. The force distribution will be somewhat inaccurate, but the error will decrease as the mesh is refined.

5 Superelement Formulations

The DBA approach uses superelements to accurately model the geometry at joints between concrete slabs. When multiple shell elements meet at a point, the implied geometry does not duplicate the actual geometry of a tapered joint. The superelement approach allows the designer to study the effect of various taper geometries and to evaluate three-dimensional (3-D) states of stress in the joints. Standard element shapes are defined parametrically, so actual structural dimensions are used to generate the refined mesh and develop the superelement stiffness matrices. The superelement formulation involves the creation of a refined finite element model consisting of solid hexahedral and prism elements. Degrees of freedom at nodes that do not interface with other elements in the structure are removed using static condensation. These are designated as slave nodes. The remaining master nodes are then constrained to mate with the 6-DOF shell nodes in the rest of the model. These procedures are computationally intensive, so a novel approach has been developed to synthesize the superelement stiffness matrix and the transformation matrix that maps the response of slave nodes to the master nodes. These matrices for an arbitrary element configuration are assumed to be linear combinations of a set of baseline matrices. The coefficients used in the linear combination are some function of the physical parameters that define the superelement, for example, length and modulus. These functions are determined by training neural networks using actual stiffness matrices.

5.1 Standard Elements

Six standard superelements have been developed. These are categorized as *point* (P1, P2, and P4) and *line* (L2, L3, and L4) elements. Figure 5.1 shows a simple structure with examples of each element type labeled.

Point elements join the corners of shells. Three types are available (P1, P2, and P4) with three, five, and eight shell nodes, respectively, depending on their location in the model. They are characterized by five parameters: depth (D), width (W), height (H), rise (S), and run (N). Figure 5.2 gives details of the characteristics of each element. The shell nodes are numbered; the parameters are defined in Figure 5.2c. These five parameters were selected to adequately model typical joint geometry. Minor approximations are made in some cases; for example, the run (N) may vary on different sides of an element. An average value is used to limit the number of parameters describing the superelement. This

method has the inherent flexibility to add parameters in order to provide more modeling options.
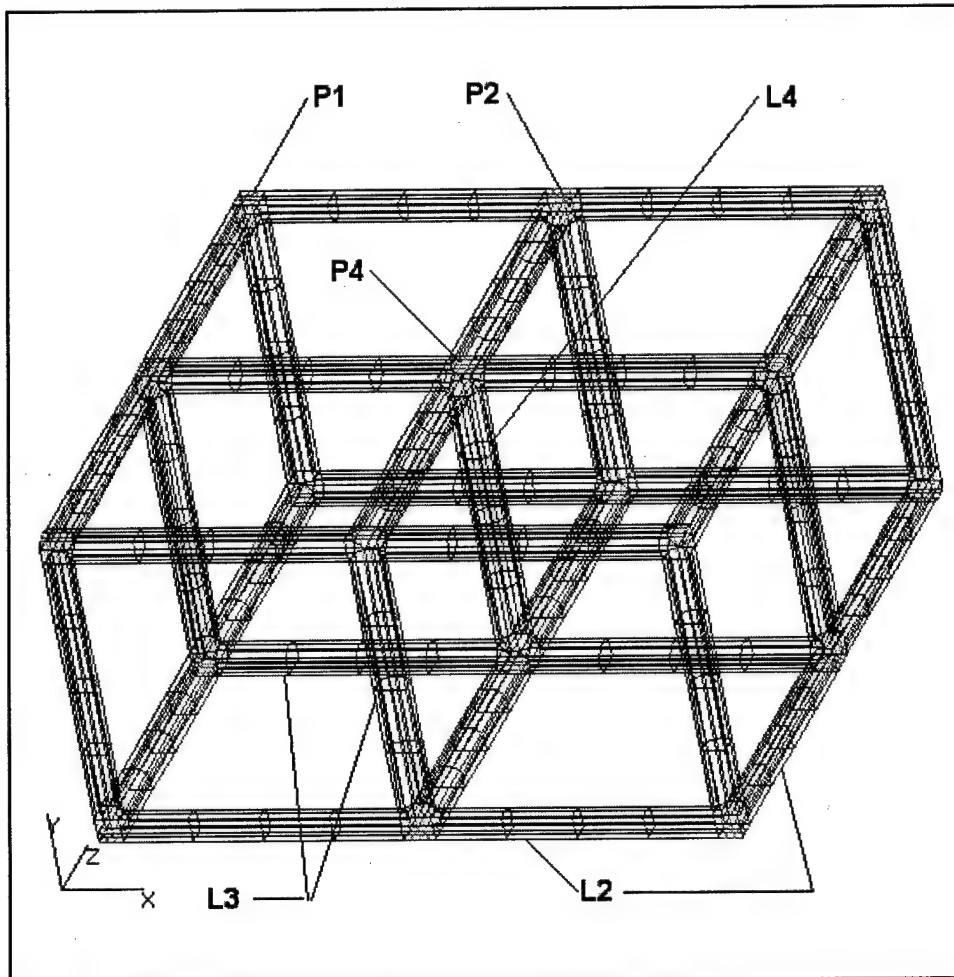

Figure 5.1. Typical superelement locations

Figure 5.3 shows the three types of line elements. These are designated L2, L3, and L4 with six, nine, and twelve nodes, respectively. They interface with two, three, or four shell elements along the sides and point elements on the ends. The midside nodes are provided for compatibility with the eight-node shell elements. The line elements are described by four parameters: length (L), width (W), depth (D), and rise (S) (as labeled in Figure 5.3c). Again, the number of parameters was limited to facilitate the development of the neural networks in the initial development of this method. In this case, rise and run are constrained to be equal on all sides of the element.
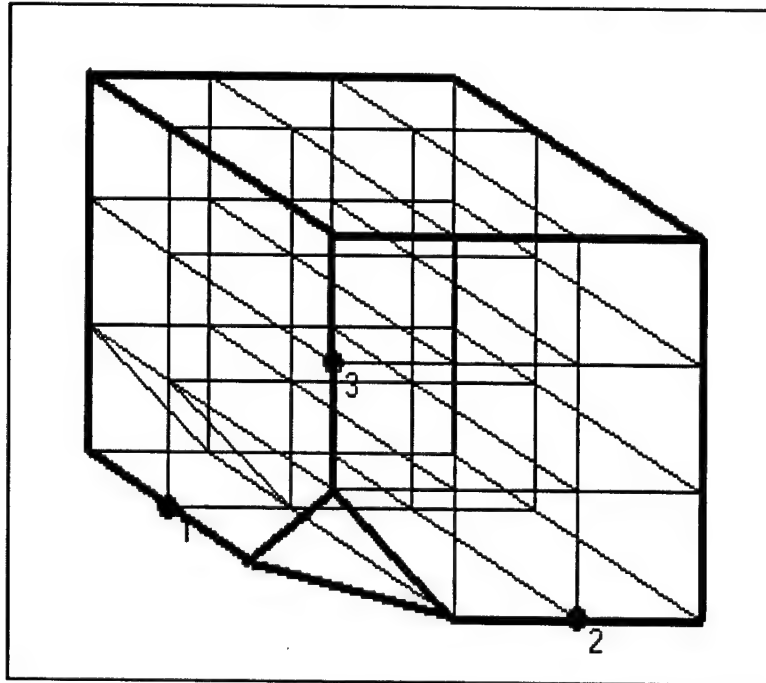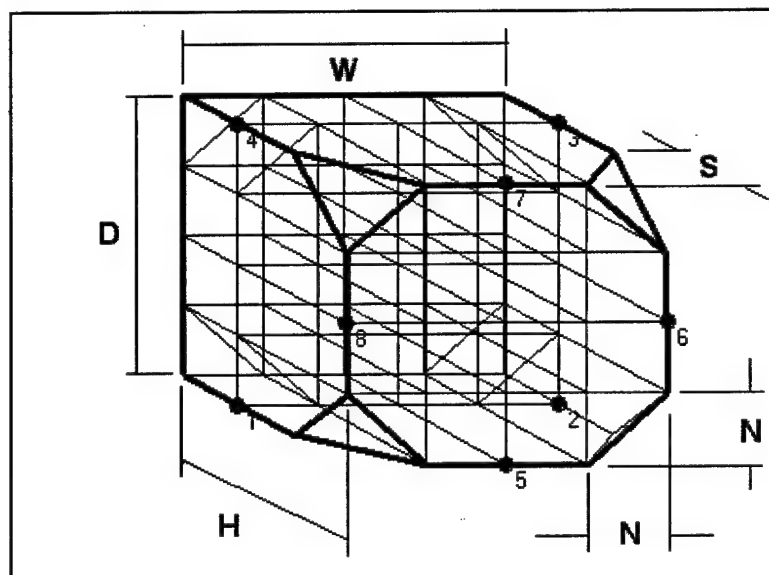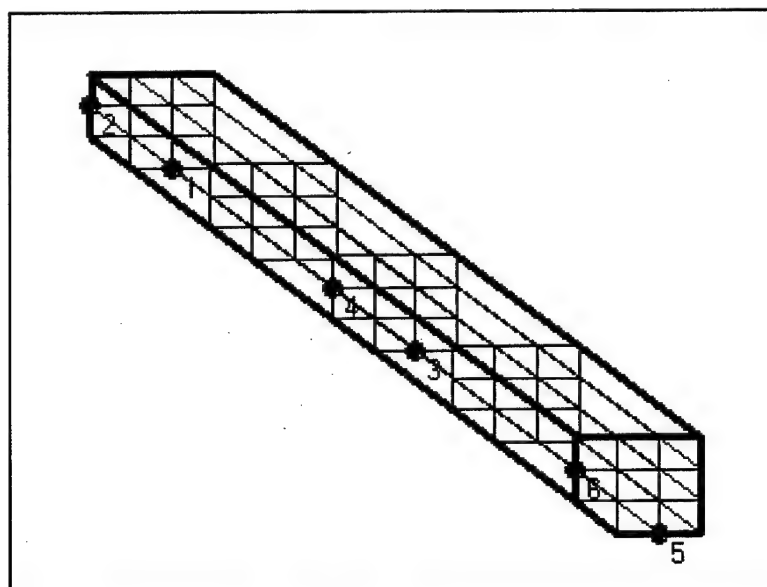
a. Point superelement P1
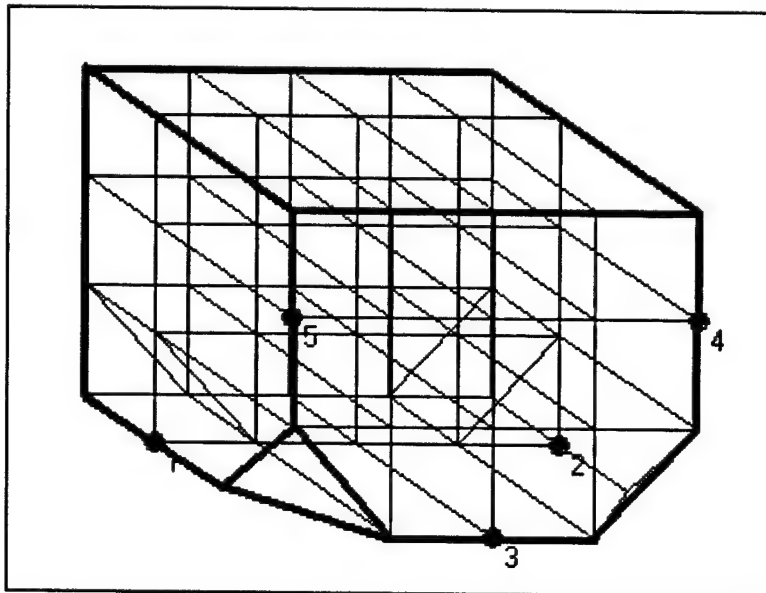
b. Point superelement P2
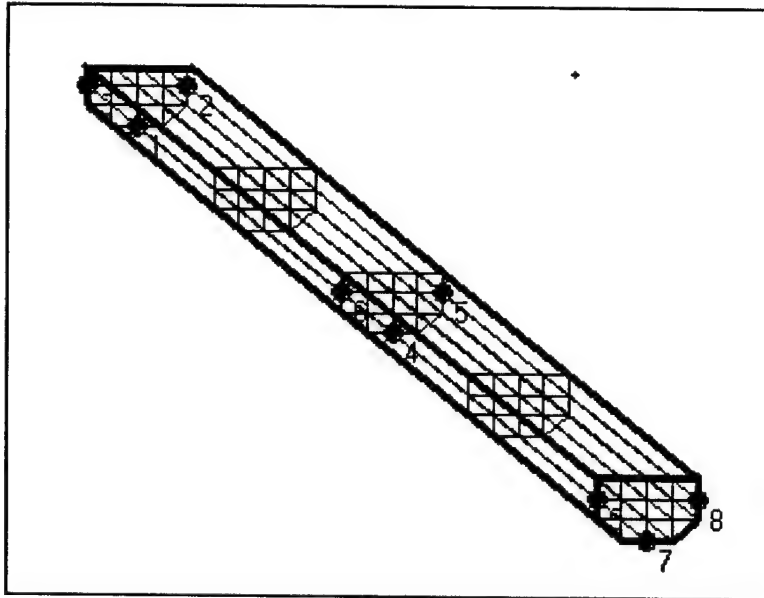
Figure 5.2. Point superelements (Continued)

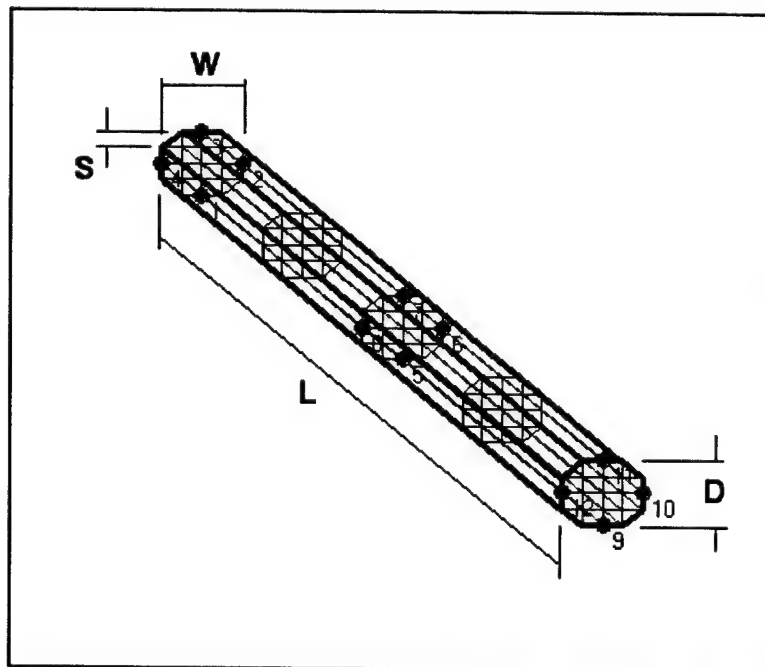c. Point superelement P4

Figure 5.2. (Concluded)

a. Line superelement L2

Figure 5.3. Line superelements (Continued)

b. Line superelement L3

c. Line superelement L4

Figure 5.3. (Concluded)

5.2　Stiffness Matrix Calculation

The calculation of the superelement matrices begins with the assembly of a conventional stiffness matrix for the solid model. A simple preprocessor is used to generate the finite element mesh for each element type. A typical coarse mesh is plotted in Figures 5.2 and 5.3 above. Standard eight-node, 24-DOF hexahedral elements are used. Prism elements with four quadrilateral and two triangular faces are created as a degenerate hexahedral element with two pairs of coincident nodes.

After assembling the stiffness matrix for the solid model, individual nodes are designated as slaves and masters. Master nodes are those on a surface that interfaces with a shell element. All other nodes are slave nodes. A Gaussian elimination procedure is applied to the stiffness matrix to create both the condensed stiffness matrix and a displacement transformation matrix (T). The procedure is documented in many finite element references (e.g., Weaver and Johnston 1984, Bathe 1982). The typical mathematical formulation involves rearranging the degrees of freedom and partitioning the stiffness matrix into slave and master submatrices.

$$[K] = \begin{bmatrix} K_{SS} & K_{SM} \\ K_{MS} & K_{MM} \end{bmatrix} \tag{5.1}$$

The [T$_{SM}$] matrix is used to calculate the deflections at slave nodes given the results at master nodes.

$$\{u_S\} = [T_{SM}]\{u_M\} \tag{5.2}$$

The [T$_{SM}$] matrix can be derived from the submatrices as

$$[T_{SM}] = -[K_{SS}]^{-1}[K_{SM}] \tag{5.3}$$

The condensed stiffness matrix is then

$$[K_{SE}] = [T_{SE}]^T[K][T_{SE}] \tag{5.4}$$

where

$$[T_{SE}] = \begin{bmatrix} -[K_{SS}]^{-1}[K_{SM}] \\ [I] \end{bmatrix} \tag{5.5}$$

and [I] is the identity matrix.

The Gaussian elimination procedure developed to create superelements generates these matrices without performing the complete inversion of [K$_{SS}$], but it is still computationally intensive.

Following the condensation, the stiffness matrix must be constrained to comply with the six-DOF shell nodes in the global finite element model. Figure 5.4 shows the master nodes on the typical line-shell element interface. The shell nodes always coincide with a master node in the line element. This node, along with the adjacent nodes on the top and bottom surface of the shell, must remain on a line to enforce a fundamental assumption in the development of the shell element.
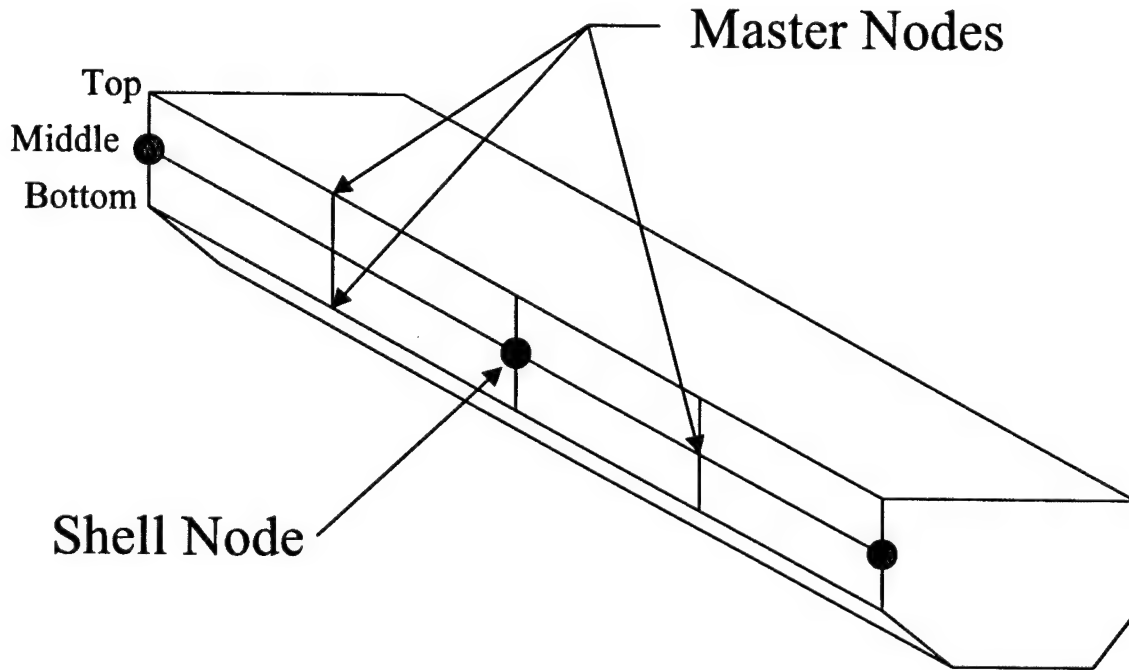
Figure 5.4. Constrain master DOF to comply with shells nodes

The transformation from shell degrees of freedom to the translational DOF of the middle, top, and bottom nodes (Figure 5.4) is

$$
\begin{Bmatrix} u_M \\ v_M \\ w_M \\ u_T \\ v_T \\ w_T \\ u_B \\ v_B \\ w_B \end{Bmatrix} = \begin{bmatrix} 1 & 0 & 0 & 0 & 0 \\ 0 & 1 & 0 & 0 & 0 \\ 0 & 0 & 1 & 0 & 0 \\ 1 & 0 & 0 & 0 & \frac{t_i}{2} \\ 0 & 1 & 0 & -\frac{t_i}{2} & 0 \\ 0 & 0 & 1 & 0 & 0 \\ 1 & 0 & 0 & 0 & -\frac{t_i}{2} \\ 0 & 1 & 0 & \frac{t_i}{2} & 0 \\ 0 & 0 & 1 & 0 & 0 \end{bmatrix} \begin{Bmatrix} u \\ v \\ w \\ \alpha \\ \beta \end{Bmatrix}
\tag{5.6}
$$

Other nodes along the interface are mapped to the shell nodes using a quadratic shape function. A transformation matrix, $[T_c]$, is developed to relate the displacement of the master nodes to the shell degrees of freedom. The final superelement stiffness matrix with shell nodes is then calculated as

$$[K_{shell}] = [T_c]^T [K_{SE}][T_c] \tag{5.7}$$

The transformations used to develop the superelement are also used for result post-processing. Displacements for the shell nodes in a superelement are extracted from the global finite element results. A transformation matrix is generated to convert these to X, Y, and Z displacements at each node in the original solid model. This matrix is formed by multiplying the $[T_{SE}]$ and $[T_c]$ matrices described above.

$$\{u_{solid}\} = [T_{SE}][T_c]\{u_{shell}\} \tag{5.8}$$

Strains and stresses are then calculated using the strain-displacement [B] matrix for the solid elements and a standard 3-D material property matrix.

5.3   Neural Network Synthesis

The development of superelement matrices is computationally intensive. A typical navigation structure model will have on the order of 1,000 superelements, so faster methods are desired. However, the ability to accurately model the true configuration and response of the structure must be maintained. Methods that allow computationally intensive operations to be performed one time during program development and make the results available in a design tool can provide an efficient approach.

The typical innovative navigation structure can be accurately modeled using the shell, point, and line elements described above. The range of sizes and shapes of these elements is somewhat restricted by the nature of the design. A catalog of elements could be developed, and the program could select the most appropriate element at run time. This approach would provide good results if enough elements are available in the catalog. However, it would be tedious and inefficient to manage the large database required, and the accuracy would always depend on how close the actual element is to a cataloged element.

It would be desirable to be able to work with a small catalog of elements and interpolate between them to form a superelement that accurately models the structure geometry. The approach developed in this research involved creating a set of N "baseline" matrices, $[K_i]$, representing the geometry of several elements throughout the parameter space. The matrices for a new superelement would be created as a linear combination of the stiffness and transformation matrices of the baseline matrices.

$$[K_{SE}] = \sum_{i=1}^{N} c_i [K_i]$$

$$[T_{SE}] = \sum_{i=1}^{N} d_i [T_i]$$

<div align="right">(5.9)</div>

Even with dozens of baseline matrices, this operation is much faster than conventional methods.

Appropriate coefficients must be calculated based on the parameters for the desired superelement. In the simple case of a one-parameter model, these could be found by calculating the value of each coefficient as a function of that parameter for several elements and then fitting a curve through those points using a regression analysis. Figure 5.5 shows a plot of a simple application of this method using linear regression. Since multiple parameters define the superelements, and the form of the function that would best fit the data is not known, a neural network approach was selected to develop this relationship. Figure 5.6 is a schematic diagram of a back-propagation neural network used to develop a function to calculate coefficients from the geometric parameters. These methods are well documented (see, for example, Fausett 1994; Hagan, Demuth, and Beale 1996; Masters 1993).

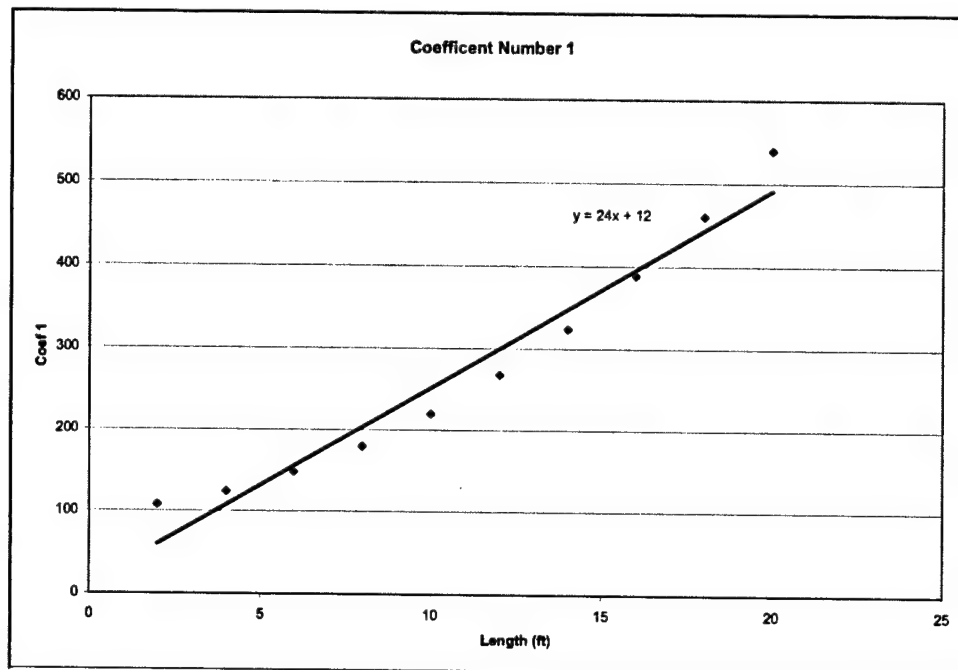Figure 5.5. Linear regression to estimate a coefficient given the length (sample)

A neural network is usually defined as an electronic circuit with many simple processors that attempts to mimic the function of the brain. It can also refer to a computer algorithm that duplicates the function of that circuit. The purpose of the network is to gain "knowledge" through experience. That knowledge is stored as
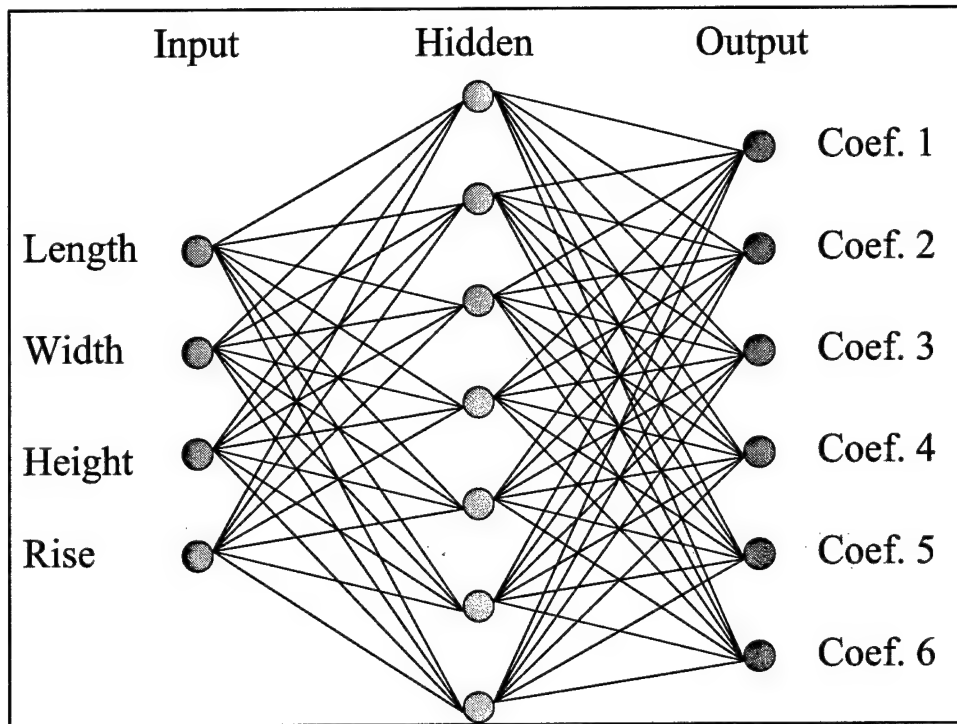
Figure 5.6. Schematic diagram of a neural network

synaptic weights. In this application, the neural network is expected to learn the values of the coefficients used in the linear combination given the input parameters. It gains experience by being fed many sets of input and output data.

The development of the neural network model is a two-step process after the baseline matrices have been determined. First, the "best" coefficient values must be calculated for several superelements, after which a neural network must be trained using these data. The coefficient values are calculated using a least-squared error approach. This is the same approach used in linear regression. In linear regression, values are calculated for the slope and y-intercept of the line that minimize the sum of the squared error between the actual data and the line. In this development, the error is the sum of the relative errors between each term in the actual matrix and the corresponding term in the linear combination,

$$\Delta^2 = \sum_{j=1}^{M}\sum_{k=1}^{M}\frac{\left\{K_{jk} - \sum_{i=1}^{N}c_i K_{i,jk}\right\}^2}{K_{jk}^{\ 2}} \tag{5.10}$$

where

        M = number of DOF in the superelement

        N = number of baseline matrices

K_{jk} = terms in the actual stiffness matrix

$K_{i,jk}$ = elements in i^{th} baseline matrix.

Partial derivatives of the error function are taken with respect to each unknown coefficient, c_i, and set equal to zero. This set of simultaneous equations is then solved to determine the coefficients. The accuracy of the matrix calculated by the linear combination is improved with more baseline matrices. The target error was an average less than 1 percent with a maximum error less than 10 percent. This was achieved with about 50 baseline matrices.

Each line in the network is assigned a weighting function that is applied to the value of the input (left) node in order to calculate the excitation at the next (right) node. One or more layers of hidden nodes are used to improve the accuracy of the model. The network must be trained in order to determine the correct weighting functions. This process requires training data derived from actual superelements. The training data are input parameter values paired with the coefficients required to calculate the superelement matrix from the linear combination of baseline matrices. Several hundred sets of data are generated to train the neural network. Initial weighting functions are arbitrarily assigned to the network.

The first set of input parameters is run through the network to calculate an approximate set of outputs. The error between the approximate outputs and the correct outputs is calculated, and the weighting functions are adjusted to reduce this error in the back-propagation phase. The sets of training data are processed through the network many times until the error is reduced to an acceptable level. The weighting functions are then stored, and this trained neural network becomes the function used to calculate the coefficients used in the linear combination to determine the superelement matrices.

6 Design Considerations

The design of innovative navigation structures is based on the requirements of ACI 318-02. Slabs are designed using the procedures for two-way slabs. Body forces are considered as dead load, and all hydrostatic pressures and concentrated loads are assumed to be live loads.

6.1 Two-Way Slab Design

The ACI 318-02 provisions for flexure design of two-way slabs as they are applied for DBA are summarized in Appendix A. When determining the minimum slab thickness (see Appendix A, Section A.6), it is assumed that walls support all slabs. In this case, the stiffness of the supporting "beam" is large, so α_m is assumed to be greater than 2 in all cases.

Since the maximum moment is expected be greater in the short direction, the reinforcement in this direction of the slab is placed at the outside on both the top and bottom with the required clear cover. Reinforcement in the long direction is on the inside, resulting in a smaller depth of reinforcement. The reinforcement in each slab is based on the worst-case combination of shear, moment, and thrust at any point in that slab for any specified load combination. As a minimum, reinforcing bars are placed at 12-in. spacing on both faces in all slabs to provide the minimum reinforcement ratio (0.0018 for Grade 60). Slabs up to 9 in. thick require No. 3 bars. Slabs between 9 and 16 in. use No. 4 bars at 12 in. The size and spacing of bars is modified based on structural requirements.

The designer provides the initial thickness of the slab. Given the moment in the short direction of the slab, designs are developed for each available bar size, since the depth of reinforcing is a function of bar size. Assuming that the largest allowable bar size should be used to minimize the number of bars in construction, the design with the largest bar size that satisfies the requirements for maximum bar spacing is selected. This bar diameter is then added to the clear cover for the design of reinforcing in the long direction of the slab, and the procedure is repeated for moments in that direction.

Stresses caused by thrust loads will tend to be much lower than those caused by flexure. ACI requirements for minimum reinforcement in walls are checked for all slabs, but it is unlikely that these will govern. A simple procedure was developed to superimpose the two cases. When the thrust is in compression, the

compressive strength of the concrete used in the flexural design calculation is reduced by the compressive stress, σ_c, factored based on wall design requirements.

$$f'_{c,reduced} = f'_c - \frac{\sigma_c}{(0.7)(0.75)} \tag{6.1}$$

When the thrust load is in tension, the reinforcement is increased in both the top and bottom of the slab to resist the additional force.

Checks are then performed to ensure that the reinforcement ratio is less than 75 percent of the balanced steel ratio in flexure. If the steel ratio is too high, the thickness of the slab must be increased. Since the design objective is a lightweight structure, the reinforcement ratio should be near the maximum.

The shear capacity of the slab is a function of thickness. It is assumed that reinforcing will be used only for shear in local areas. This shear capacity is factored and compared with the shear at every analysis point.

$$\phi V_c = (0.85)2\sqrt{f'_c}bd \tag{6.2}$$

The factor of safety (F.S.) must be greater than 1 at all points in the slab.

$$F.S. = \frac{\phi V_c}{V_{FE}} \tag{6.3}$$

where V_{FE} is the shear load per foot determined from the finite element analysis, and the width, b, is 12 in. This procedure takes advantage of the finite element results to develop a simpler algorithm, but it is consistent with the assumptions in ACI 318.

6.2 Superelement Analysis

The use of superelements in the joints of the structure permits the designer to study the stresses in more detail. In the typical design, the required reinforcing for the slabs is extended into the joints, and some additional reinforcing is added to the tapered regions. DBA methods have not been developed to detail joint reinforcing.

6.3 Controlling Case Determination

The design of a slab is based on the reinforcing requirements at the critical point in the slab for all load cases. Each slab must be checked for all load cases. The case requiring the most reinforcement in each of the four layers will govern.

6.4 Automatic Design Modification

An initial slab thickness must be proposed by the designer in order to analyze the structure. The initial design is based on these analysis results. These results will suggest changes to the design in some situations. One goal in the design is to produce the lightest structure that meets all requirements. A second goal is to produce a constructible design that allows for reuse of formwork and reinforcing schedules that are easy to fabricate. The automatic redesign procedures developed for DBA are based on these two goals.

Designs are screened to identify slabs that may be overdesigned. These are slabs with a high factor of safety for shear and a low reinforcement ratio. The thickness of these slabs is reduced in 1-in. increments and redesigned based on the shear, moment, and thrust values from the initial analysis. Although this is not exact, small changes in thickness will have little effect on these results. If the design for this thinner section is acceptable, the slab thickness is changed in the design. The thickness is further reduced and the redesign calculations are repeated until an unacceptable design is produced.

Similarly, automatic redesign procedures increase the thickness of slabs that are underdesigned. The shear factor of safety is less than 1 in these slabs, the steel reinforcement ratio is greater than the allowable, the thickness is insufficient to construct the slab given the required reinforcement, or the thickness is less than the minimum allowed for serviceability by ACI 318.

7 Shear, Moment, and Thrust Calculation

Design and analysis methods for concrete structures are based on the shear, moment, and thrust (axial forces) actions on the beam, wall, or slab section. Various methods are available to approximate these actions. The finite element method is used in this development.

The design of innovative navigation structures is concerned with ensuring that the thickness and reinforcement in the slab sections is adequate to resist the applied loads. These sections are treated as two-way slabs in the design. Stresses can be calculated in the joints, but design criteria are not as well established when the overall response is more complex than simple bending actions. The superelement approach developed in this research allows the designer to evaluate these stresses. Capabilities are also included to evaluate overall bending action in a cross section of the structure.

7.1 Shell Elements

Methods for calculating shear, moment, and thrust in shell elements are well established. Because the individual stress components will be used in later cross-section plots, these were also calculated. Actions in each shell element are evaluated by extracting the nodal displacements from the global finite element results. The global rotations (α_G, β_G, and γ_G) are transformed back to the local (α and β only) system. The strain-displacement [B] matrix (Equation 4.12) is then evaluated at each integration point in the local coordinate system and used to calculate the six local strain components at the bottom ($\zeta = -1$) and top ($\zeta = +1$) of the element. Stresses are then determined from the strains and used to calculate the moment, shear, and thrust at the integration points. Since the stress results are aligned with the local shell element coordinates, this calculation is straightforward.

Defining the element coordinates as 1 and 2, the shear, moment, and thrust in the 1 direction can be determined from the extensional stress in that direction and the shear stress in the 13 plane. Actions in the 2 direction are derived from stresses in that direction (Figure 7.1). Assuming that the stress varies linearly
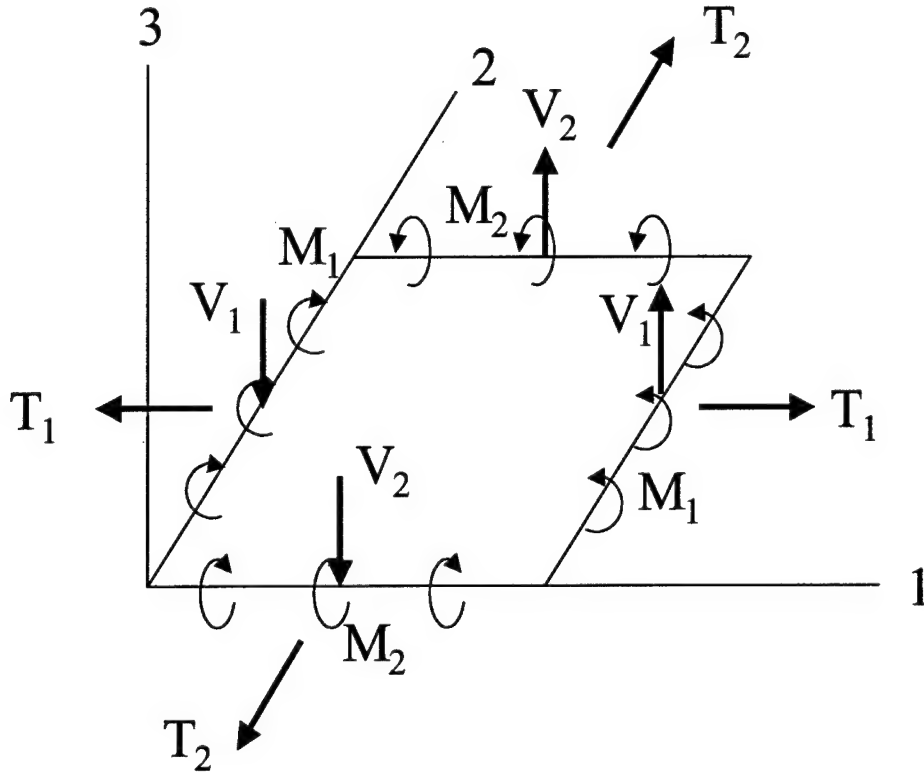
Figure 7.1. Actions in terms of local axes for a shell element

through the thickness, the thrust component is a function of the average of the stresses on the top and bottom. This average stress is multiplied by the thickness to determine the thrust per unit length. If the thrust component is removed from the stress distribution, the resulting stress is pure bending. The moment per unit length is then simply a function of the maximum stress. Finally, shear per unit length is computed from the appropriate shear stress component by multiplying by the thickness. The actual, parabolic shear stress distribution cannot be calculated in a standard shell element because the derivation is based on the assumption that plane sections remain plane; however, the calculation of total shear is accurate. Figure 7.2 shows the derivation of thrust and moment.

Once shear, moment, and thrust are calculated at the integration points, they are extrapolated to the nodes based on linear shape functions. Essentially, a four-node, bilinear element is constructed with the integration points as the corners. The standard shape functions for this element are used to extrapolate to the nodes in the shell element. For example, Node II in Figure 7.3 is at $r = \sqrt{3}$ and $s = -\sqrt{3}$. The actions at Node I (A_I), given the values at the four integration points (A_1, A_2, A_3, and A_4) shown in Figure 7.3, are given as

$$A_I = \sum_{i=1}^{4} A_i N_i \tag{7.1}$$

Shell
Stresses

$$\sigma_{Thrust} = \frac{\sigma_{x'Top} + \sigma_{x'Bot}}{2}$$

$$Thrust \, / \, foot = (\sigma_{Thrust})(Thickness)$$
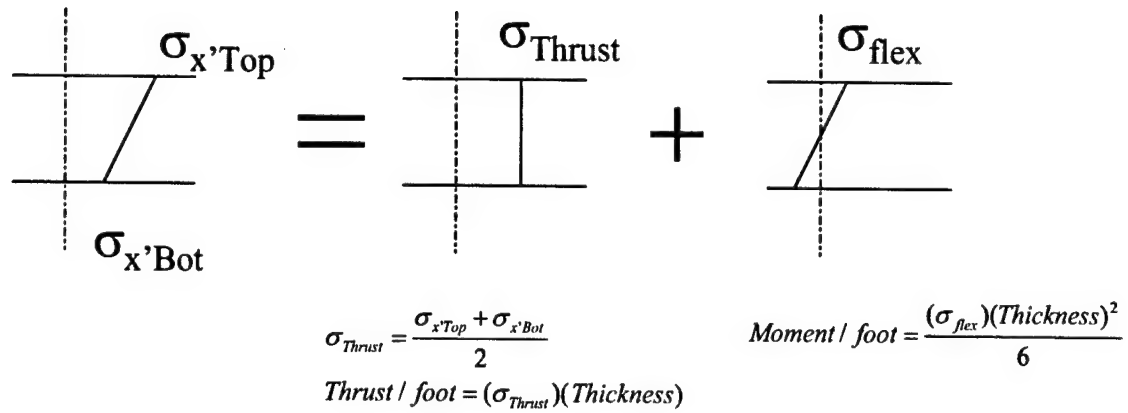
$$Moment \, / \, foot = \frac{(\sigma_{flex})(Thickness)^2}{6}$$

Figure 7.2. Calculate moment and thrust from shell stresses
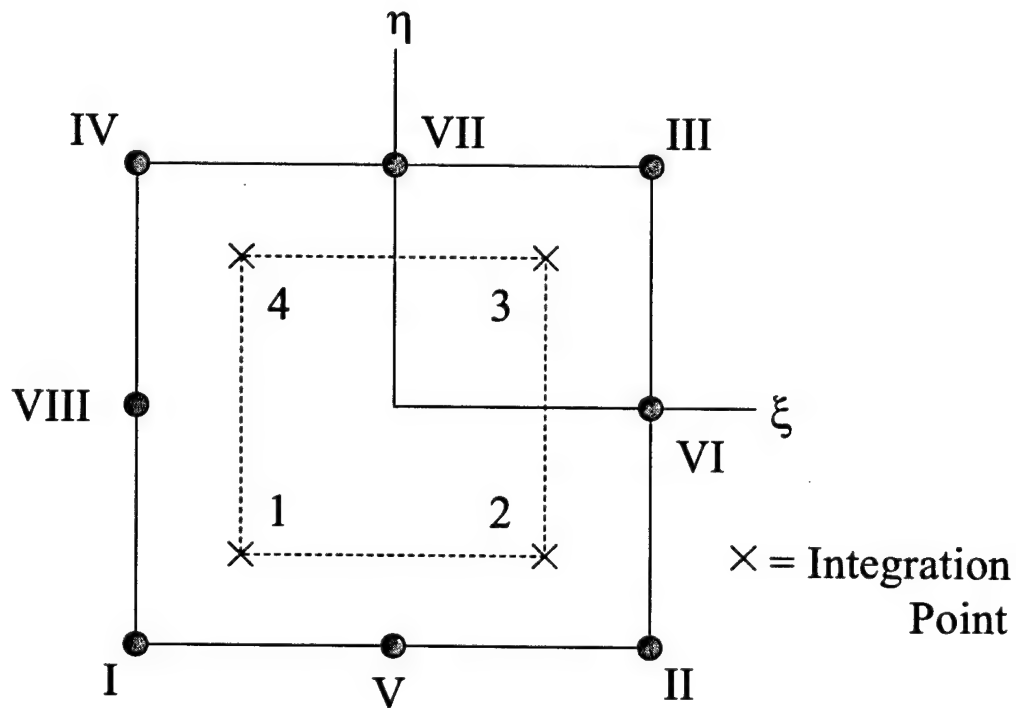

Figure 7.3. Extrapolate results at integration points to nodes

where

$$N_1 = 0.25(1-r)(1-s)$$
$$N_2 = 0.25(1+r)(1-s)$$
$$N_3 = 0.25(1+r)(1+s)$$
$$N_4 = 0.25(1-r)(1+s)$$

and

$$r = \sqrt{3}\xi, \quad s = \sqrt{3}\eta$$

7.2   Stress Contour Calculation

Stresses can also be calculated at selected cross sections in the model. Cross sections will pass through both shell elements and superelements. The stress calculation is different for each case. When a section is cut along a numbered or lettered section line, the shells are cut though the midplane. The shell element stresses at the midplane are derived from the shear and thrust values calculated earlier by dividing the traction per unit length by the thickness. These values are transformed to the global coordinates using the direction cosines at the node. Moment values do not affect stresses at the midplane.

When sections are cut normal to a shell element, stresses are also derived from the shear, moment, and thrust values, but the two-dimensional (2-D) cross section must be constructed from the shell element nodal coordinates and the thickness information. A pseudo-element is constructed with the shell nodes on the midplane and new nodes on the top and bottom surfaces at each shell node, as shown in Figure 7.4. Stress values at these nodes are calculated by, essentially, inverting the procedure used earlier to calculate the shear, moment, and thrust from the nodal stresses.

Where cross sections are cut through superelements, the strains and stresses are calculated from the nodal deflections of the original solid model and the strain-displacement matrices of the hexahedral and prism elements. The nodal deflections are calculated by transforming the deflections of the shell nodes calculated in the global finite element model, as described above. The cross sections are forced to fall on element boundaries, so the strains and stresses calculated at the nodes of the solid element become nodal values for the 2-D quadrilateral element that appears in the cross section.

7.3   Shear, Moment, and Thrust Diagrams

Once stresses on a cross section have been determined, shear, moment, and thrust can be calculated on any plane through the section by numerically integrating the stresses. The appropriate stress values are calculated at all element

boundaries intersected by the plane and assumed to vary linearly across the element.
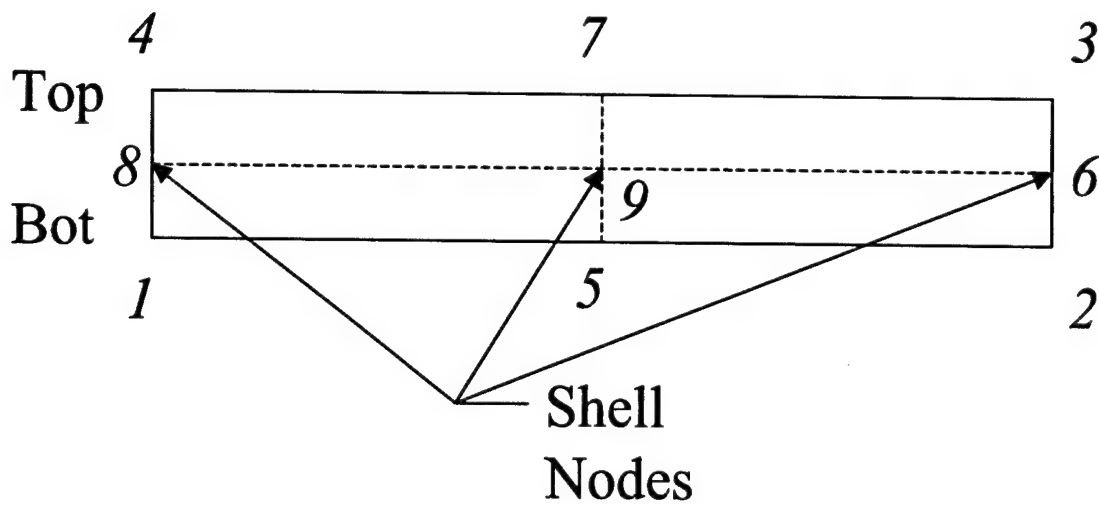

Figure 7.4. Pseudo-element for evaluating shell stresses

For example, Figure 7.5 shows the extensional stresses in the horizontal direction for a typical section. Three finite elements were intersected by the vertical line at $X = 3.7$. The thrust in the X direction is determined by calculating the net area enclosed by the stress plot. The stress accounted for by the thrust is then subtracted from the extensional stresses. The approximate neutral axis can be determined from these adjusted values. Moment is then calculated by adding the contribution of each area of the stress plot multiplied by the distance to the neutral axis. Values can be calculated at several points along the horizontal axis to construct a moment diagram.
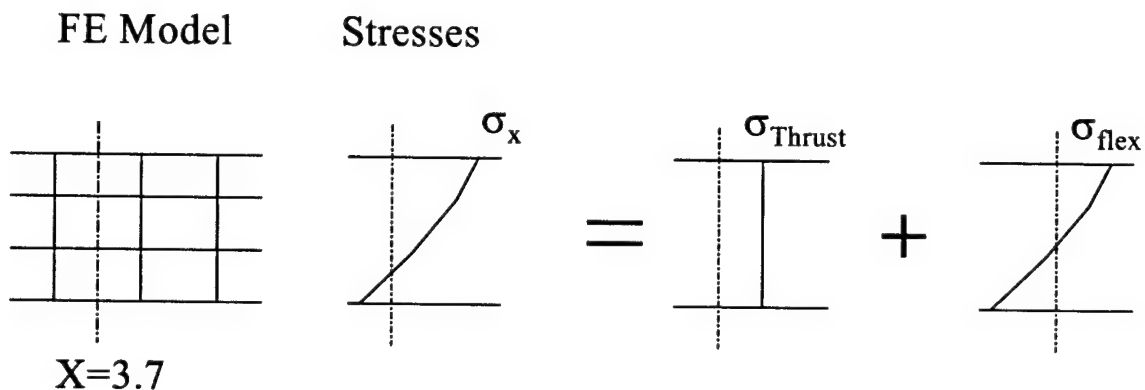

Figure 7.5. Calculation of thrust and moment from cross-section stresses

8 Soil/Pile Modeling

8.1 Modeling Assumptions

During initial fabrication, the structure is supported on the soil in the dry dock. After the structure is placed on its underwater foundation, it is supported by a combination of piles and/or drilled piers, and the grout pumped under the structure. The nature of the support condition will affect the response of the structure. The soil or grout is modeled as an elastic foundation under the shell elements. The supporting piles or drilled shafts are assumed to be rigid in the vertical direction, but lateral stiffness can be estimated and accounted for in the DBA analysis.

8.2 Soil Stiffness

The formulation for modeling shells on an elastic foundation is summarized in Chandrupatla and Belegundu (1997). The formulation assumes that the soil response is linear elastic. The designer must know the stiffness of the soil in place, that is, the amount the soil deflects vertically when subjected to a uniform pressure. The units for this stiffness are pressure divided by distance, for example, 100,000 psf/ft (or 100 kips/ft^3). This property is related to the modulus of vertical subgrade reaction, K_v, described by McCarthy (1998). Values for a 1-sq ft plate range from 100 to 700 kips/ft^3 depending on the soil type. The actual settlement is a function of the size of the foundation and is greater for larger foundations—approaching 4 times the settlement of the 1- sq ft plate with equal pressure. The effects of time-dependent response should also be considered when selecting this value.

8.3 Pile Stiffness

Methods for calculating pile stiffness have been developed by the Corps of Engineers' CASE Project (Office, Chief of Engineers 1983). These methods are based on the stiffness of the actual pile or drilled pier, the stiffness of the surrounding soil or bedrock, and the type of interaction assumed between the pile and the soil.

References

American Concrete Institute (ACI). "Building code requirements for structural concrete and commentary," ACI 318-02, Farmington Hills, MI.

Bathe, K.-J. (1982). *Finite element procedures in engineering analysis.* Prentice Hall, Englewood Cliffs, NJ.

Chandrupatla, T. R., and Belegundu, A. D. (1997). *Introduction to finite elements in engineering*, 2d ed. Prentice Hall, Englewood Cliffs, NJ.

Fausett, L. (1994). *Fundamentals of neural networks: Architectures, algorithms, and applications.* Prentice Hall, Englewood Cliffs, NJ.

Hagan, M.T., Demuth, H. B., and Beale, M. (1996). *Neural network design*, PWS Publishing, Boston, MA.

Masters, T. (1993). *Practical neural network recipes in C++.* Academic Press, New York.

McCarthy, D. F. (1998). *Essentials of soil mechanics and foundations.* Prentice Hall, Englewood Cliffs, NJ.

Office, Chief of Engineers. (1983). "Basic pile group behavior," Technical Report K-83-1, CASE Task Group on Pile Foundations, U.S. Army Engineer Waterways Experiment Station, Vicksburg, MS.

Weaver, W., Jr., and Johnston, P. R. (1984). *Finite elements for structural analysis.* Prentice Hall, Englewood Cliffs, NJ.

Appendix A
Design Algorithms

[Reference: ACI 318-02, Chapters 13 and 14]

A. Flexure Design of Slabs:

1. This procedure applies for design of slab systems reinforced for flexure in more than one direction, with or without beams between supports.
2. This procedure excludes one-way slabs and soil-supported slabs.
3. Moments are determined using finite element analysis.
4. The maximum specified f_y is 60,000 psi in shells and plates.
5. Determine all the data for the analysis: f_y, f'_c, b, L.

(Initially assume $b = 1$ ft to compute area of reinforcement A_s per foot of slab.)

L

b

Plan View
Slab

6. Determine the minimum slab thickness, h:

    ✓ Two-way slab: Ratio long/short span •2 ($b \leq 2L$).

    ✓ Minimum thickness for the slab supported with beams on all sides, no interior beams. For minimum thickness, a calculation is necessary to calculate the moment of inertia of the slab and beams. ACI 318 specifies that where beams include portions of the slab as flanges, the length of the flange has to equal h_w or $4*h$ (in.), whichever is smaller, as shown in the following figure:

Portion of the slab
included as beam
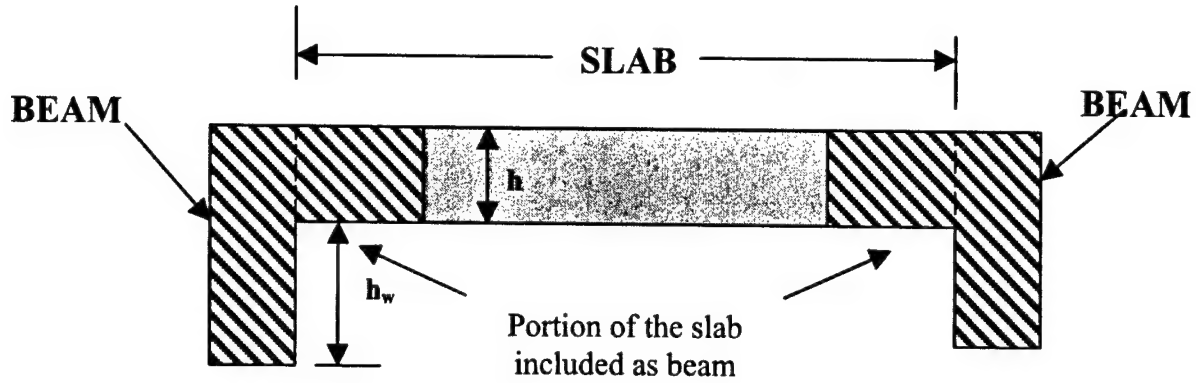
✓ This portion is considered in the moment of inertia calculation. Using the moment of inertia of each section (slab and beam) in both directions, α is calculated for both directions as

$$\alpha_{1,2} = \frac{E_b * I_b}{E_s * I_s}$$

✓ where E_b and E_s represent the modulus of elasticity of the beam and of the slab, respectively, and I_b and I_s represent the moment of inertia of the beam and of the slab, respectively. After α_1 and α_2 are determined, α_m is calculated as

$$\alpha_m = \frac{\alpha_1 + \alpha_2}{2}$$

✓ The minimum thickness depends on this α_m value. If α_m is equal to or less than 0.2, use

$$h_{s\,min} = \frac{l_n * \left(0.8 + \left(\dfrac{f_y}{200,000} \right) \right)}{36}$$

where l_n (in.) is the clear span of the slab, and f_y is in pounds (force) per square inch. For α_m greater than 0.2 but not greater than 2.0, use

$$h_{s\,min} = \frac{l_n * \left(0.8 + \left(\dfrac{f_y}{200,000} \right) \right)}{36 + 5 * \beta (\alpha_m - 0.2)}$$

and for α_m greater than 2.0, use

$$h_{s\,min} = \frac{l_n * \left(0.8 + \left(\frac{f_y}{200,000}\right)\right)}{36 + 9 * \beta}$$

7. Cover and effective depth, d. Assume bars from following:

    ✓ For spans up to 20 ft: generally use No. 4 bars.

    ✓ For spans up to 25 ft: generally use No. 5 bars.

    ✓ For span over 25 ft: generally use No. 5-6 bars.

    ✓ The clear cover (cc) for concrete exposed to weather conditions:

        • For No. 5 bars and smaller: minimum cc = 1.5 in.

        • For larger bars, minimum cc = 2 in.

    ✓ Using these assumptions, **d** can be estimated for various bar diameters (d_b) as

        • For the long span of a flat plate or slab:

            d = h − cc - 1.5*d$_b$

        • For the short span of a flat plate or slab:

            d = h − cc − 0.5*d$_b$

8. Compute **a** and the reinforcement area **A$_s$** (slab with beams):
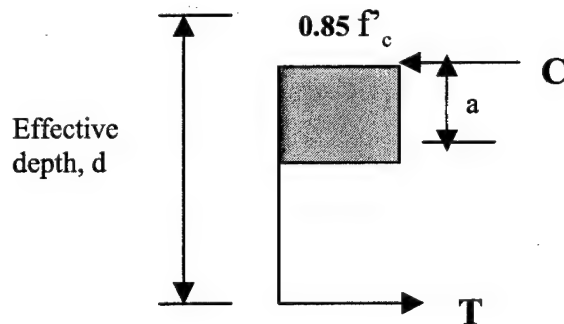
$$T = A_s * f_y \quad\quad\quad\quad\quad (1)$$

$$C = 0.85 * f'_c * a * b \quad\quad\quad\quad\quad (2)$$

$$M_n = T (d - a/2) = A_s * f_y (d - a/2) \quad\quad\quad\quad\quad (3)$$

✓ Solving for **a** in Equations 1 and 2 by equilibrium **T = C**:

$$a = A_s * f_y/(0.85 * f'_c * b) \qquad (4)$$

✓ Solving for **As** in Equation 3:

$$A_s = M_n/[f_y * (d - a/2)] \qquad (5)$$

✓ Assuming an **a**, calculate A_s from Equation 5.

✓ With the value of A_s obtained, calculate **a** from Equation 4.

✓ Continue the iterations (calculating A_s and **a**) until the calculated **a** from Equation 4 is almost equal to **a** calculated in the last iteration.

9. Check $A_{s\,(min)}$:

✓ $A_{s\,(min)}$, the minimum reinforcement for the slab, should be at least the minimum amount for shrinkage and temperature reinforcement:

- Slabs where Grade 40 or 50 deformed bar is used **0.0020**
- Slab where Grade 60 deformed bars or welded wire fabric (plain or deformed) is used **0.0018**
- Slabs with reinforcement yield stress exceeding 60,000 psi measured at a yield strain of 0.35 % is used ....**(0.0018 * 60,000)/f_y**

Note: the ratio of reinforcement area to gross concrete area cannot be less than 0.0014.

- $A_{s_{min}} = \rho * b * h$

- If $A_s > A_{s\,(min)}$, $\rho > \rho_{min}$

- If not, use $A_{s\,(min)}$ as A_s, and check M_n for that A_s (Step 8).

- Calculate **a** if A_s changes, as

$$a = (A_s * f_y)/(0.85 * f'_c * b)$$

and the new ρ:

$$\rho = A_{s\,(min)}/(b*h)$$

✓ If A_s does not change, calculate

$$\rho = A_s/(b * h)$$

10. Check if ρ is less than **0.75** ρ_{bal} (f_y and f'_c in psi):

✓ $\rho_{bal} = [(0.85* {}_1 * f'_c)/f_y] * [87,000/(87,000 + f_y)] \backslash$

- for concrete strength $f'_c \leq$ **4000 psi,** ${}_1 =$ **0.85**
- for f'_c between **4,000** and **8,000 psi,**

  ${}_1 =$ **1.05 – 0.05*(f'_c/1000)**

- for f'_c greater than **8,000 psi,** ${}_1 =$ **0.65**

✓ Calculate:

0.75 ρ_{bal}

✓ For $\rho < \rho_{bal}$, $f_s = f_y$, and **a** is sufficient. If $\rho > \rho_{bal}$, the slab would fail in compression with $f_s > f_y$. Start the procedure again and recalculate **a** (increase **b** or **d**).

✓ Check if ρ is less than **0.75** ρ_{bal}:

- If $\rho <$ **0.75** ρ_{bal}, ρ is less than the maximum value

  allowed by ACI.

11. Compute M_n and M_u:

✓ $M_n = A_s * f_y * (d - a/2)$

✓ $\varphi M_n = 0.9*M_n$

✓ **Check with the factored ultimate moment, M_u:**

  (M_u was determined from finite element analysis)

- If $\varphi M_n > M_u$, proceed.

- If $\varphi M_n < M_u$, stop. A_s is too small, increase A_s and start

  again.

12. Determine the A_s total by multiplying it by **b** (total length in feet).

13. With the total A_s and the bar diameter, select the numbers of bars (**n**)

  to use in the design.

14. Spacing for the reinforcement A_s:
  ✓ The spacing for the reinforcement A_s for the two-way slab at
    the critical sections shall not exceed **2*h**
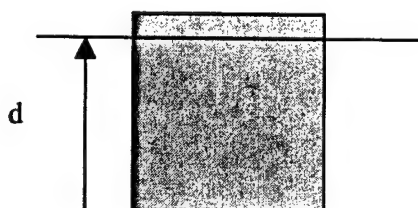
✓ Maximum spacing for shrinkage and temperature reinforcement bars:
  - Shall not exceed **3*h** (thickness of slab, inches)
  - Shall not exceed **18 in.**

15. Calculate the mean spacing in the slab by
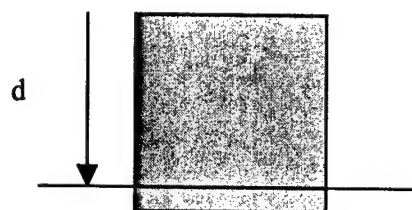
$$S = b \text{ (total, in.)}/n \quad (S < 2^*h)$$

16. Repeat the procedure for maximum positive and negative moments.
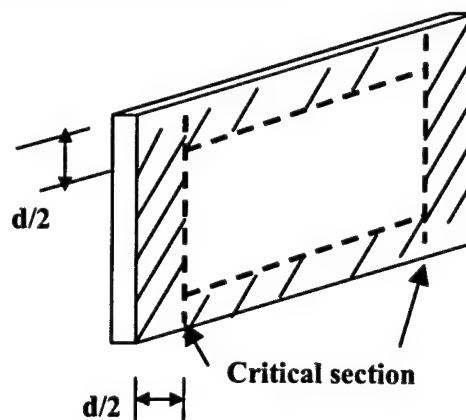
Negative moment

Positive moment

17. For negative moment, d is calculated in the same way as for positive moment.

B. Shear Design of Slabs:

1. Determine the shear from finite element analysis.
2. For shear design, it is necessary to consider the behavior of slabs failing in one-way shear and in two-way shear.
3. It is important to determine the location of the critical perimeter.

Critical section

4. One-way shear:

- $V_c = 2\sqrt{f'_c}\, b_w\, d$ **(use the greater d from positive or negative moments in each direction)**

5. Two-way shear:

   ✓ Take the smaller of

   - $V_c = [2 + (4/\beta_c)] \cdot f'_c\, b_0\, d$

   - $V_c = (_s\, d)/(b_0 + 2) \cdot f'_c\, b_0\, d$

   - $V_c = 4 \cdot f'_c\, b_0$

   - Where

     $\beta_c =$ ratio of long side to short side of column, reaction area or concentrated load.

     $_s =$ 30 for edges columns

     $b_0 =$ perimeter of the critical section

6. Calculate the allowable shear for both two- and one-way shear:

   (V_u was determined from finite element analysis)

   - $V_c = 0.85 * V_c$

7. Check for two-way shear and for one-way shear:

   - Check with the factored ultimate shear, V_u:

   - If $\varphi V_c > V_u$, proceed. If $\varphi V_c < V_u$, stop. The shear capacity can be increased by increasing the b_0, and by adding shear reinforcement. Use closed stirrups with bars in all four corners. The stirrups are designed as for a beam, and must be extended at least as far as the critical section on which $\varphi V_c > V_u$ (one-way shear). These stirrups are not practical for slabs less than about 12 in. thick. Two different sizes of stirrups are required to fit between the layers of flexural reinforcement in the two directions. They must be spaced at d/2, which requires a large number of stirrups.

C. Design of Walls:

1. Minimum thickness of walls:

   ✓ Exterior basement walls and foundation walls: should not be less than 7.5 in.

   ✓ Bearing walls should not be less than 4 in. or L/25, where L is the supported height or length, whichever is shorter.

2. Reinforcement in walls:

   ✓ Minimum vertical and horizontal reinforcement ratio:

      • Vertical:

         (a) Deformed bars not larger than No. 5 with yield strength not less than 60,000 psi...0.0012

         (b) Other deformed bars 0.0015

      • Horizontal:

         (a) Deformed bars not larger than No. 5 with yield strength not less than 60,000 psi...................0.0020

         (b) Other deformed bars 0.0025

3. Calculate the minimum area of reinforcement in each direction:

   ✓ $A_{s\min\_vertical} = \rho_{min} * h * B$ for vertical direction

   ✓ $A_{s\min\_horizontal} = \rho_{min} * h * L$ for horizontal direction

4. Calculate the axial capacity load as

   ✓ $\varphi Pn = 0.8 * \varphi * \left[0.85 * f'_c * \left(A_g - A_{st}\right) + f_y * A_{st}\right]$

   ✓ A_g is the gross area of section in that direction, in.^{2}

   ✓ A_{st} is the reinforcement steel in that direction, in.^{2}

5. Check if $\varphi P_n \geq$ Pu. If not, increase A_{st} or h.

6. Calculate the shear capacity of the wall (kips):

   ✓ $d = 0.8 * l_w$ (l_w in inches). ACI uses this value as the effective depth for horizontal shear forces.

   ✓ $V_c = 2 * \sqrt{f'_c} h * d$.

   ✓ If $V_c < V_u$, shear reinforcement is needed.

7. Shear reinforcement shall be provided as

   ✓ $V_s = \dfrac{A_v * f_y * d}{s2} \le 8 * \sqrt{f'_c} * b_w * d$

   ✓ $A_v = \dfrac{\left(0.75 * \sqrt{f'_c} * b_w * s\right)}{f_y} \ge \dfrac{50 * b_w * s2}{f_y}$

   ✓ $\varphi V_n = \varphi * \left(V_c + V_s\right) \le 10 * \sqrt{f'_c} * h * d$

   ✓ Check if $V_n \ge V_u$. If not, add more shear reinforcement.

8. Spacing limit for vertical, horizontal, and shear reinforcement, s:

   ✓ Shall not exceed: $d/2 \le 24$ in.

   ✓ Horizontal shear reinforcement spacing: shall not exceed $l_w/5$, $3*h$ or 18 in. (l_w is the horizontal length of wall).

   ✓ Vertical shear reinforcement spacing: shall not exceed $l_w/3$, $3*h$ or 18 in.

9. Development length for bars and hooked bars for each direction:

   ✓ The greater of $12d_b$ or d (effective depth at each direction).

   ✓ Hook length will be $12d_b$.

REPORT DOCUMENTATION PAGE

1. REPORT DATE *(DD-MM-YYYY)*	2. REPORT TYPE	3. DATES COVERED *(From - To)*
August 2003	Final report	

4. TITLE AND SUBTITLE	5a. CONTRACT NUMBER
Design by Analysis of Innovative Navigation Structures; Theoretical Manual	5b. GRANT NUMBER
	5c. PROGRAM ELEMENT NUMBER

6. AUTHOR(S)	5d. PROJECT NUMBER
Kerry T. Slattery, Guillermo A. Riveros	5e. TASK NUMBER
	5f. WORK UNIT NUMBER
	33273

7. PERFORMING ORGANIZATION NAME(S) AND ADDRESS(ES)	8. PERFORMING ORGANIZATION REPORT NUMBER
Southern Illinois University, Carbondale, IL 62901; U.S. Army Engineer Research and Development Center Information Technology Laboratory 3909 Halls Ferry Road Vicksburg, MS 39180-6199	ERDC/ITL TR-03-4

9. SPONSORING / MONITORING AGENCY NAME(S) AND ADDRESS(ES)	10. SPONSOR/MONITOR'S ACRONYM(S)
U.S. Army Corps of Engineers Washington, DC 20314-1000	11. SPONSOR/MONITOR'S REPORT NUMBER(S)

12. DISTRIBUTION / AVAILABILITY STATEMENT

Approved for public release; distribution is unlimited.

13. SUPPLEMENTARY NOTES

The companion to this report is ERDC/ITL TR-03-5, "Design by Analysis of Innovative Navigation Structures; User Manual."

14. ABSTRACT

This report describes the development of design by analysis methods for innovative navigation structures. The modeling approach is designed to facilitate the development of a complex three-dimensional finite element mesh and efficiently analyze the structure. Techniques to automatically generate a detailed model of the structure and perform required analysis and design calculations for the individual concrete slabs under all applied loads are illustrated, along with methods for identifying and reporting details of the design for each slab under the worst-case loading.

The two-way slab design approach (based on American Concrete Institute guidance, ACI 318-02) is summarized, along with a description of methods to calculate shear, moment, and thrust throughout the shell elements and at selected cross sections of the superelements. The design section includes the approach used to modify design parameters based on analysis results. Finally, guidelines are provided for modeling the response of soil and piles used in the foundation.

15. SUBJECT TERMS		
Finite element methods Hydrostatic loading	Plates and shells Pontoon structures Reinforced concrete	Thin-wall panels Two-way slabs

16. SECURITY CLASSIFICATION OF:			17. LIMITATION OF ABSTRACT	18. NUMBER OF PAGES	19a. NAME OF RESPONSIBLE PERSON
a. REPORT	b. ABSTRACT	c. THIS PAGE			19b. TELEPHONE NUMBER *(include area code)*
UNCLASSIFIED	UNCLASSIFIED	UNCLASSIFIED		56	